FINAL REPORT

NASA GRANT NsG-428

SEPTEMBER 1966

DEPARTMENT OF PHYSICS

GEORGETOWN UNIVERSITY

WASHINGTON, D.C.

TABLE OF CONTENTS

PART II

FIGURES

Papers Removed

LIST OF FIGURES

1. Introduction

The work done during the final year of Grant NSG-428 was concerned to a large extent with detailed examination of electroluminescent materials, i.e., their optical, electrical, and magnetic properties. In addition, some work was done on the thermal control of temperatures of spacecraft surfaces by means of electro-optical crystals. As the larger part of this report is concerned with electroluminescence, some of the standard concepts and definitions of this field will be reviewed below.

Luminescence includes all forms of light emission in which kinetic heat energy is not essential for the mechanism of excitation [1]. Crystalline luminescent solids are usually referred to as phosphors. By electroluminescence (E.L.) is meant the emission of light from a phosphor resulting from the application of an electric field. Light output may occur for either d.c. or a.c. fields. In the following, we will only be concerned with the latter case.

The action of electric fields upon microcrystals embedded in an insulator was first reported by Gudden and Pohl [2] in 1920. They observed a momentary enhancement of the afterglow from a phosphor previously irradiated by ultraviolet radiation. However, the sustained emission of light by phosphor powders embedded in an insulator was first reported by Destriau [3] in 1936.

Since the light output occurs in the visible part of the spectrum, it is clear that the emission process must involve electronic transitions rather than merely rotations or librations of molecules or vibrations of crystals (phonons) and molecules. As a result, it is convenient to divide the problem of understanding the mechanism of E.L. into several parts relating to (1) the excitation process, (2) the life history of electrons in excited states, and (3) the de-excitation of the sample by means of either phonon and/or phonon

emission. Valuable information may also be obtained by studying the decay of efficiency, i.e., the ratio of light output and power input as a function of time.

PART I

Investigation of ZnS:$MnCl_2$ Phosphors

Chapter I - Techniques of Preparation

a) Preparation of Phosphors

Zinc sulfide, which is sufficiently doped with certain purities, will exhibit electroluminescence. These impurities may be activators such as Cu, Ag, Mn, and Pb, which are capable of supplying electrons to the crystal, or they may be co-activators such as Cl, Br, and I, which are capable of receiving an electron in order to attain a more stable configuration.

The starting material for this study was Sylvania zinc sulfide phosphor, lot ZC-1131. The sizes of the phosphor particles ranged between ten to twenty microns. The powder was snow white, as is characteristic of zinc sulfide in extremely pure form. A chemical analysis was performed on the phosphor by the Schwartzkopf Microanalytical Laboratories of New York City. No trace of copper, manganese, or chlorine was found by their analysis, which was capable of detecting one part per million of these elements.

The impurities were introduced by wetting the zinc sulfide with a solution containing manganous chloride salt (Fisher Scientific USP grade). Five strengths of solutions containing from 10^{20} $MnCl_2$ molecules per c.c. to 10 MnCl molecules per c.c. were prepared with deionized water.

The salt was weighed out using an analytical balance which was accurate to within 0.1 mg. For the 50 ml flasks used, this error corresponds to 6×10^{14} molecules per c.c., or six parts per million for the strongest solution. The weaker solutions were then prepared by

diluting the stronger ones to avoid the weighing of an extremely small amount of salt. It was possible to measure solution volumes to within 0.01 ml, which represented a .0041% error in initial concentration of doped material. The impurity solution and zinc sulfide powder were thoroughly mixed and were placed in an oven at 125°C until dry. The impurities were then present in the form of a coating around the phosphor grains.

It was assumed that the amount of $MnCl_2$ which diffused into the zinc sulfide was proportional to the amount originally added. This assumption is based on Fick's law of diffusion which relates the net flux J of atoms of one species in a solid to the gradient of the concentration N of this species[4].

$$J = -D \text{ grad } N \qquad (1)$$

where D is a function of temperature.

The diffusion of these impurities into the crystals was accelerated by firing the mixture at high temperatures. The temperature dependence of D takes the following form:

$$D = D_o \exp[-H/kT] \qquad (2)$$

where T is the absolute temperature, H is the activation energy for the process, and D_o is the diffusion constant.

Experimental procedures similar to those developed by Lehmann[5] were adopted. An oven temperature of 950°C was chosen for the firing of the phosphors. A half gram of sulfur was added to the phosphor prior to each firing since Wachtel[6] had observed that this enhanced

electroluminescence. Since oxygen quenched electroluminescence [7], a dry nitrogen atmosphere was used for firings of the phosphors.

The phosphor was placed in a quartz firing tube with a close fitting cap. This quartz capsule was then lowered into a ceramic mullite tube. Dry nitrogen was circulated through the tube prior to, and during, firing. The diffusion oven employed for the firings was cylindrical in shape, 13 inches long, and 1.6 inches in diameter. A Keithley electrometer (Model 400) was used to monitor a thermocouple which was placed at the center of the oven. The powder was fired in 10 gm portions to insure uniformity. After 90 minutes, the mullite tube was removed from the oven and allowed to cool. The powder was removed, crushed, and another half gram of sulfide was added. The entire firing procedure was then repeated.

The powder was washed with deionized water to remove any of the excess $MnCl_2$ which resided on the surface. These ions produce surface conduction in the presence of high fields and decrease the efficiency of electroluminescence in the crystal volume [8]. The phosphor was then dried, crushed, and sieved. Phosphor particles ranged in size between 20 and 40 μ.

Chemical analyses were also performed on two of the doped powders. In both cases 30% of the $MnCl_2$ had diffused into the ZnS. It was assumed that this was approximately the case for all the powders. Fifty grams of each concentration of powder were prepared. Roughly, one gram of powder was necessary to make one cell. Powders were stored in a desiccator until used in the preparation of electroluminescent cells.

b) Construction of an Electroluminescent Cell for Optical Measurements

A parallel plate capacitor construction[9] with the phosphor powder suspended in a dielectric between two electrodes was adopted. The basic design of the electroluminescent cells is shown in Figure 1. A plexiglas plate 2" x 2" x 3/8" served as a substrate material. A transparent electrode of stannic oxide was deposited on the plates by the supplier, Grimes Zep Aero Corporation.

Several dielectric materials were tested including clear lacquers, water glass, silicone dielectrics and resins, and clear enamels. Dupont Dulux Enamel, RK 190-clear, was finally chosen for several reasons. It was resistant to penetration by water vapor and had a high breakdown strength (1000 volts across a 1.0 mil layer). Its glossy finish provided a regular surface for deposition of the gold electrode. The enamel did not react with the phosphor and remained stable under repeated application of high fields.

Five grams of phosphor were mixed with each 10 ml of enamel. Since the enamel was 60% volatile, the ratio of phosphor volume to dielectric volume was about three parts enamel to one part phosphor. The phosphor grains were suspended in the clear enamel which hardened when sprayed on the plexiglas substrate. This resulted in a good mechanical bond of the dielectric layer to the transparent conducting layer.

In order to develop high fields within the phosphor with moderate applied voltages, the thickness of the dielectric layer was kept small. On the other hand, for uniformity of illumination and to eliminate the possibilities of shorts through the ZnS crystals, the thickness should be large compared with the size of the crystals. A compromise was made

between these conflicting requirements. The average thicknesses of cell dielectric layers varied between 1 and 3 mils. The change in thickness over the surface of a given sample was controlled to within one tenth of a mil. This represented a variation of 10% to 3.3%, depending on thickness of the dielectric layer.

A gold electrode was then evaporated onto the dielectric layer. Gold was chosen since it was a good electrical conductor which was chemically inert. A bell jar chamber, which was evacuated by means of a mechanical pump in series with an oil diffusion pump, was used for the gold evaporations. The cells were masked prior to the evaporation of the gold in order to prevent shorting of the two electrodes.

Electrical contacts were made to the electrodes by means of washers, nuts, and screws. It was observed that the humidity in the air produced a rapid deterioration of the electroluminescence of the cells. The detrimental effects of water vapor on electroluminescent cells had been recognized by Roberts [10]. Therefore, all cells were sealed with a layer of Castelite thermosetting plastic.

The phosphor containing 10^{16} $MnCl_2$ molecules per c.c. was observed to be quite poor in quality and was eliminated from the test. Approximately 30 cells were made from each concentration of phosphor, or about 125 cells in all.

Cells were also made from the pure Sylvania zinc sulfide taken directly from the shelf. Although chemical analysis had not detected any traces of Mn or Cl impurities greater than one part per million, it was not known what level of impurity contamination was necessary to produce electroluminescence. The host material itself should not exhibit

any electroluminescence if meaningful results were to be obtained. Also, in order to investigate the role of thermal dislocations in electroluminescence, the pure zinc sulfide was fired in the normal manner and cells were then constructed.

As discussed in Chapter IV. a), it is not feasible to use samples of this type for EPR measurements. For this reason it was decided to produce cells of a cylindrical type which differed from the above mentioned form for two reasons. Firstly, in order to retain a good loaded quality factor for the microwave cavity, all materials introduced into it should have as low a loss tangent as possible and, secondly, the samples themselves should have a volume which is small compared to that of the cavity. Both objectives were satisfied by the following construction. The phosphor powder was sprayed onto non-magnetic metal wires with dimensions of .06 - .08 inches diameter and a length of about 10 inches. The second electrode was again obtained by evaporating a layer of not more than .001 inches of gold onto the phosphor containing dielectric. The thickness of the gold layer is somewhat critical since radiation at optical and microwave frequencies must be capable of transmitting it. Figure 1a is a schematic of this cell; however, it is not drawn to scale. Since cylindrical cavities were used for the entire EPR investigation, the cell could be placed along the cavities' axis without ruining either the quality factor or changing the frequency of the cavity unduly.

Chapter II - Optical and Electrical Measurements of ZnS:$MnCl_2$ Phosphors

Although the spectra of ZnS phosphors do not show any structure and are therefore not useful for investigation of details of the electron kinetics, it is still possible to obtain some understanding of the processes involved in the transfer of electrons and their de-excitation. To this end, a variety of properties of ZnS phosphors of different impurity concentration were measured as a function of voltage and frequency.

a) Spectral Composition of Emission

First the spectrum of the phosphors was taken for a variety of voltages and frequencies. The equipment used for this purpose was a monochrometer of the Fastie-Ebert type. The mirror had a focal length of 30 inches and the grating was 3 inches wide with a total of 90,000 lines. The detector was a photomultiplier tube of the type Dumont 6292, whose output was amplified and recorded on a Moseley Autograph, Model 680M, recorder. The transmission coefficient of the whole system was calibrated with a tungsten standard lamp (N.B.S. - QL 161).

The cells were excited with an audio oscillator (Hewlett-Packard, Model 200AB) whose output was amplified (McIntosh, Model 40) and stepped up by a transformer (UTC Type LS 52) to yield rms voltages of up to 1200 volts. A sketch of the experimental arrangement is depicted in Figure 2.

The output intensity is plotted as a function of wavelength for a variety of frequencies in Figure 3. There appear two peaks, one at 4750Å, the other one at 5800Å. It is to be noted in particular that the blue peak increases with increasing frequency while

the yellow one reverses itself. No such effect was observed for constant frequency and variable voltage, as shown in Figure 4. In order to ascertain how the bands change as a function of applied frequency, the output over appropriate wavelength bands was measured. Figures 5 and 6 show the transmission characteristics of the filters and the experimental arrangement, respectively. The results are shown in Figure 8. While the blue band increases monotonically up to a frequency of about 8 Kcps, the yellow peak shows a clear peak at about 3.2 Kcps. It should be noted that although there is no justification to talk in terms of a blue peak, the output of the blue band does indeed decrease beyond 8 Kcps. A study of the brightness (intensity) as a function of applied voltage followed the well known equation [11,12]

$$B = B_0 \exp(-A/\sqrt{V}) \qquad (1)$$

where both B and A are constants. It is possible to assign frequency independent values to A if measured individually for the two bands. Figure 7 is a plot of (1), i.e., the log B versus $1/\sqrt{V}$ for three different concentrations. It is seen clearly that B does indeed obey (1) over more than two periods. When measuring the values of A as a function of impurity concentration and applied frequency, it turned out that except for minor variations only two distinct numbers could be obtained, Table I, one for either band. These were $A = 80.2 \pm 4.8$ for the blue and $A = 67.5 \pm 3.5$ for the yellow band. Several authors [13,14,15] reported in the past that A is frequency dependent. However, this conclusion was drawn from the measurement of the total brightness. It is clear that on the basis of the

evidence presented above, we could interpret our results in the same manner. On the other hand, it appears to be somewhat more reasonable to define two frequency independent values for A, each one associated with one band and possibly with one activation center or one de-excitation process.

In order to check whether the frequencies corresponding to the maximum output of the two bands are field dependent, several runs were made to determine the brightness as a function of either one variable. The results are presented in Figure 9, which shows that there is no field dependence of the optimum frequency.

b) Brightness Waves

Still another approach to the problem consists in a detailed examination of brightness waves. By this is meant a study of the light output in time as a sinusoidal voltage is applied to the sample. One observes most often two output peaks for each half cycle of the voltage wave (16). Of interest is the relative change of the phases of voltage, current, and light output. Since this problem was investigated elsewhere*, we concentrated on only a few aspects of this phenomenon.

The experimental setup is presented in Figure 10 and the brightness waves obtained for voltages of 150V rms and a variety of frequencies are reproduced in Figure 11. As the frequency is increased from 50 cps to 5 Kcps, two peaks are observed - the first one decreasing with frequency and the second one increasing with frequency (17). By the use of filters, it was determined that the blue emission was located in the second peak while the yellow emission was distributed

*E. Conway, Dissertation, Georgetown University (to be published).

TABLE I

SLOPE OF BRIGHTNESS-VOLTAGE CURVES
AS A FUNCTION OF FREQUENCY AND
IMPURITY CONCENTRATION

Impurity Concentration $MnCl_2$ molecules per cm^3	Slope A of Brightness-Voltage Curve							
	Yellow Emission				Blue Emission			
	.5Kc	1Kc	5Kc	10Kc	.5Kc	1Kc	5Kc	10Kc
10^{17}	75.7	83.2	78.6	80.8	66.0	64.4	67.5	68.0
10^{18}	76	80.2	77.2	79.0	69.7	67.5	70.1	68.3
10^{19}	81.3	85.0	81.5	79.8	67.2	68.5	65.3	67.0
10^{20}	79.6	80.9	82.0	80.6	66.2	67.8	68.0	66.7

over both peaks (Figure 12). Repeating these measurements for different voltages showed that the shape of the output wave did not change. The intensity of course did, according to Eq. (1).

c) Aging of Cells

In spite of the fact that ZnS phosphors have been investigated very intensely, there still remain a large number of very basic questions to be answered. One of the reasons for this situation is, apparently, the fact that phosphors age [17], i.e., they lose their ability to emit light. On the one hand, this effect makes it difficult to compare results from different laboratories. On the other hand, it is clear that just this type of behavior might give important information about the E.L. process itself. Since the changes occur over long periods of time they can easily be investigated. One interesting feature of this aging process is that it only occurs while the sample is excited. In this type of measurement it was particularly important to protect the cells against moisture since it is known to accelerate the aging process [18].

The deterioration of samples was studied as a function of frequency, applied voltage, and impurity concentration. The luminescence appeared to decrease in three steps - a brief, rapid exponential decrease, - a somewhat slower decay exponential - and then a very gradual leveling off period. Since it is known that phosphors exhibit hysteresis effects [19] care has to be taken that all cells to be compared are freshly constructed. Figure 13 shows a typical decay curve for various voltages at 1000 cps for 230 hours running time.

It was found that for a given frequency and concentration, the rate of decay was essentially independent of the applied voltage. Figure 14 shows the decay of four samples of the same concentration at 3000 cps. As can be seen, their rates of decay were the same within experimental error. However, the frequency of the applied voltage greatly influenced the rate of decay. Figure 15 shows the initial change in brightness for five similar samples at different frequencies. Some authors have found that the decay was a linear function of the total number of cycles which the cell had experienced. This was not found to be the case here, but it was found that the decay rate decreased with increasing concentration of impurities. In particular, it was found that the brightness decrease during the second stage of the decay process could be represented by the equation

$$B = \frac{B_0}{1 + {}^{t}/_{\tau_{1/2}}} \qquad (4)$$

where $\tau_{1/2}$ is the period during which the brightness decreases by a factor of two. The pertinent results are presented in Tables 2 thru 5. Figure 16 shows $\tau_{1/2}$ for different frequencies and impurity concentrations.

If one assumes that the decay is due to an annealing process that eliminates E.L. centers, then the fact that the process is voltage independent indicates that a diffusion process takes place which is concentration controlled while the applied field merely triggers the process.

TABLE II

AVERAGE DECAY HALF-LIFE OF BRIGHTNESS
AS A FUNCTION OF FREQUENCY AND
IMPURITY CONCENTRATION

Impurity Concentration	Half-Life of Decay (Minutes)				
	.5Kc	1Kc	3Kc	5Kc	10Kc
$10^{17} MnCl_2/cm^3$	750	300	150	90	55
$10^{18} MnCl_2/cm^3$	980	350	170	115	65
$10^{19} MnCl_2/cm^3$	---	420	225	130	80
$10^{20} MnCl_2/cm^3$	---	520	300	170	95

TABLE III

DECAY TIMES T_1 AND T_2 AS A FUNCTION OF VOLTAGE AND IMPURITY CONCENTRATION

Cell Type Impurities/cm^3	Voltage (rms volts)	Thickness of Cell (mils)	Decay Times (Minutes) T_1	T_2
10^{17}	200	1.4	32	300
	200	1.7	33	286
	300	1.3	30	300
	300	1.5	31	330
10^{18}	200	1.5	31	350
	200	1.4	30	345
	300	2.1	32	365
	300	2.0	33	340
10^{19}	200	1.5	29	415
	200	2.1	31	400
	300	2.0	30	450
	300	1.7	31	415
10^{20}	200	1.5	34	560
	200	2.1	31	510
	300	1.7	30	520
	300	2.1	32	500

TABLE IV

DECAY HALF-LIFE OF YELLOW EMISSION AS A FUNCTION OF FREQUENCY AND IMPURITY CONCENTRATION

Cell Type Impurities/cm^3	Cell Voltage (rms volts)	Decay Half-Life (Minutes		
		1Kc	5Kc	10Kc
10^{18}	200	375	125	80
	400	360	120	80
10^{19}	200	445	150	105
	400	430	155	100
10^{20}	200	540	225	120
	400	530	215	125

TABLE V

DECAY HALF-LIFE OF BLUE EMISSION AS A FUNCTION OF FREQUENCY AND IMPURITY CONCENTRATION

Cell Type Impurities/cm	Cell Voltage (rms volts)	Decay Half-Life (Minutes)		
		1Kc	5Kc	10Kc
10^{18}	200	280	70	40
	400	255	60	35
10^{19}	200	340	85	50
	400	320	75	40
10^{20}	200	410	125	60
	400	390	105	55

d) Relaxation Times

Observations were made of the cells under pulsed d.c. excitation. When a square wave pulse is applied to an electroluminescent cell, two pulses of light emission are generally observed [20]. One appears upon the application of the external field and the other upon the removal of that field.

The light output was studied as a function of time for various square wave frequencies and amplitudes. Figure 17 shows a block diagram of the experimental apparatus. The output of the electroluminescent cells was monitored by a phototube (RCA 7265) whose signal was displayed on an oscilloscope, externally triggered by the square wave generator. Photos taken of decay traces were analyzed and output vs. time curves were plotted.

It was found that the light output as a function of time could be expressed as follows:

$$I = I_1 e^{-t(1/\tau_1)} + I_2 e^{-t(1/\tau_2)} \qquad (5)$$

A typical semilog plot of brightness vs. time is shown in Figure 18. The lower curve was obtained by subtracting the upper line from the output curve. From these graphs the values of τ_1 and τ_2 could be obtained.

Filters were used to study the decay of the yellow emission and the blue emission separately. Testing was done at low frequencies (20 to 100 cycles) since low repetition rates were necessary to observe the decay. No variation of τ_1 or τ_2 was observed outside of experimental error. For the yellow emission τ_1 was

efficiencies were always found in the region below 100 cycles. Unfortunately, brightness at these frequencies was generally very poor. It should be noted that only those cells whose light output had sufficiently stabilized were employed for these relative efficiency measurements.

Absolute efficiencies were measured by using an Eppley thermopile (Model 6010) with a response of .16 mv per watt/cm^2 of incident radiation. A potentiometer (Honeywell-Rubicon, Inc.-Model 2768) was used to measure the putput of the thermopile. A power meter Fluke-Model 102) was used to measure input power to the cells. Figure 21 shows a block diagram of experimental apparatus.

Absolute efficiencies ranging from 0.1% to 2.3% were measured. Electroluminescent emission from the cells was on the order of .01 mw/cm^2. Lowest efficiencies occurred at very low or very high voltages and at very high frequencies. Nothing which could be interpreted as a resonance effect was observed. The optimum frequency of operation was judged to be near 500 cycles, where both brightness and efficiency were reasonably high. The choice of operating voltage depended on cell thickness, impurity concentration, frequency, and previous aging of the cell.

f) Microscope Observation

The electroluminescent cells were observed with a low power microscope (30 power). Emission occurred only in a relatively small percentage of the crystals, perhaps 10%. The emission appeared as dots of light which were randomly scattered over the cell surface. As the applied voltage was increased, the light output from these dots became more intense and, also, new emitting areas appeared. As the

frequency was increased, the areas of light emission became more sharply defined and blue emitting areas became very intense light emitters.

The blue and yellow emission originated in different locations in the cell and appeared to be independent of one another. It was not possible to observe any electroluminescent lines or striations of light due to internal reflection and light scattering. These had been reported in recent literature (21,22).

g) Electrical Characteristics

Cells were constructed by sandwiching a dielectric layer between two conducting electrodes so that it was expected that they should behave electrically as a resistor-capacitor combination. Thus, any anomalous behavior could be interpreted as effects produced by the phosphor grains in the dielectric layer.

The resistance of the cells was greater than 500 megohms so that no direct currents were detectable through the cells. However, alternating currents were observed to increase as a linear function of frequency (Figure 22). The phase angle between the current and voltage was always found to lie between 90° and 86°.

The equivalent circuit for the electroluminescent cells was established from the above data. A resistor R in parallel with a capacitor C possesses the electrical characteristics which were observed for the cells. For such a circuit

$$\frac{1}{Z} = \frac{1}{R} + j\,C \qquad (6)$$

where Z is the impedance of the parallel combination.

found to be 0.10 ± .01 msec and τ_2 was 0.47 ± .05 msec. For the blue emission τ_1 was measured to be 0.10 ± .02 and τ_2 was measured to be 0.97 ± .06 msec. Figure 19 shows a typical scope trace of light output vs. time for a square wave applied to an electroluminescent cell. The inaccuracies involved in the photographic technique are responsible for the rather large deviations of the measured relaxation times.

Care must be taken to separate d.c. and a.c. effects here. Some samples which conduct a.c. currents were found to exhibit constant yellow emission during the entire duration of the applied square wave. This was superimposed on the emission which occurs when the field is applied and removed, which made analysis difficult.

e) Efficiency Measurements

The efficiency of electroluminescence is of interest from both fundamental and practical viewpoints. The efficiency for an electroluminescent cell is defined as the ratio of the light output power to the electrical power input. In general, maximum light output and maximum efficiency can not be obtained simultaneously.

Relative efficiency measurements were taken to determine the voltage and frequencies at which maximum efficiency occurred. Absolute efficiencies were measured to obtain a rough idea of the probability of phonon emission relative to phonon emission in the process.

Relative efficiencies were measured using the apparatus in Figure 6 to which a power meter (Fluke-Model 102) was added. Figure 20 shows a typical efficiency vs. frequency curve. Peak

The current I which will flow when a voltage V is applied is then

$$I = \frac{V}{Z} = \frac{V}{R}(1 + j\omega CR) \tag{7}$$

Since the resistance R is extremely large, Eq. (7) can be approximated by the expression

$$I = j\omega CV \tag{8}$$

This predicts that the current will be a linear function of frequency and will be 90° out of phase with the applied voltage so that it describes the electrical behavior of the electroluminescent cells.

Power consumption for a typical sample was a few tenths of a watt. Figure 23 shows the variation in electrical power input as a function of applied voltage frequency. The input power was measured by a Fluke power meter (Model 102).

It was previously established that the cells age more rapidly at high frequencies. Attempts have been made to explain this decay in terms of frequency effects [23,24]. However, it seemed that the input power to the sample might be an important factor in the decay process. Figure 23 shows the rapid increase in the input power as the frequency increases. This energy must be dissipated in the crystal and could serve to trigger decay mechanisms.

h) Characteristics of Undoped Phosphors

Chemical analysis had shown that the host Sylvania zinc sulfide was essentially free from impurities. However, as a precautionary measure, cells were made from the undoped, unfired powder to see if any electroluminescence might be detected. No electroluminescent output was observed. The sensitivity of the phototube was sufficient to detect 10^{-12} watts of radiation.

Next, the undoped powder was prepared in exactly the same manner as the doped powders except for introduction of impurities. These cells exhibited a faint blue electroluminescence which increased with frequency and voltage. Lack of sufficient intensity prevented the measurement of the spectral emission. However, the relaxation times of the blue light were measured. The output was found to decay, as predicted by Eq. (5).

$$I = I_1 e^{-t(1/\tau_1)} + I_2 e^{-t(1/\tau_2)} \qquad (5)$$

The values of τ_1 and τ_2 obtained were $\tau_1 = 0.19 \pm .04$ msec and $\tau_2 = 1.10 \pm .08$ msec. These times would seem to indicate that the blue emission observed in the undoped powder may be due to the same mechanism responsible for the blue emission in the doped powders. Also, it was considered significant that the blue emission was produced by heating impurity free ZnS to a sufficiently high temperature. The intensity of this light appeared to depend on the introduction of atomic sulfur into the phosphor prior to firing. Alexander, et al.[25], had noticed a blue emission in ZnS after firing but did not link it with sulfur. Zinc vacancies were postulated as the blue luminescent center. However, the introduction of the impurities appears to enhance this blue emission.

Chapter III - Discussion and Interpretation of Results

a) Basic Theory of Electroluminescence

For reasons of completeness, we start our discussion with a brief elementary review of accepted ideas on electroluminescence. In a crystal, certain allowed energy states are available for electron occupation as a result of the crystalline potential. The introduction of impurities perturbs the potential function and introduces new allowed energy states. When transitions involving these states yield visible radiation, a luminescent center is said to be present.

To explain luminescence, only dipole radiation need be considered since the emission probability for the various multipole orders decreases by a factor of approximately $(a/\lambda)^2$ each time the multipole order changes by one. Here a is the source dimension and λ is the wavelength of emitted radiation. For visible luminescence ($\lambda = 5000\text{A}^{\circ}$) from atoms ($a = 1\text{A}^{\circ}$), the factor a/λ is 1/5000. Thus, quadruple and higher order radiations are negligible compared with dipole radiation.

To obtain electroluminescence, the electrical energy from the applied field must be converted into visible radiation. In general, this conversion process will involve three separate processes [26]. Initially, an electron must be excited, directly or indirectly, by the applied field. Secondly, the excited electron may be transported through the crystal to a region of de-excitation. Finally, the de-excitation occurs with subsequent emission of radiation. These processes are generally described by means of the band theory model or the configuration coordinate model.

The band theory model [27] is based on the general quantum mechanical treatment of the interaction of valence electrons with the three dimensional periodic potential of the crystal lattice. When individual atoms are brought

together to form a crystalline lattice, the characteristic energy levels of the individual atoms are broadened into bands of allowed energies which may or may not overlap. The introduction of impurities into a crystal often produces allowed energy states between these bands. Just as the electrical properties of semiconductors are dominated by impurities, the luminescent properties of phosphors are dominated by localized activator and trapping states in the forbidden band.

A composite band theory analysis of luminescence is shown in Figure 24. In general, an electron can be excited either from the valence band or from an impurity level to the conduction band. Both the positive hole and the excited electron may migrate through the lattice until emission occurs. The electron then falls back down to either the activator level or the valence band. The wavelength of the emission is determined by the difference in energy levels. Between excitation and emission, trapping may occur. Electron traps are shallow levels in the forbidden band in which conduction electrons may reside temporarily.

The principal limitation of the band model is that the particular energy band and levels are characteristic of a particular crystalline configuration. As a result, atomic rearrangements that occur during luminescence are ignored. Thus, the model does not indicate the origin of the large quantum difference between absorption and emission energies. Also, it does not suggest the pronounced broadening of excitation and emission energies with temperature. The band theory model is especially suitable for interpreting luminescence phenomena involving the transport of electrons through the lattice. If the absorption and emission processes involve transitions between states peculiar to the activator ion, the energy bands of the lattice are not involved so that another model must be applied.

The configuration coordinate model[28] emphasizes atomic rearrangements. In order to describe transitions and rearrangements occurring in luminescent phenomena, a useful simplification is to define a center. The center is the ion undergoing electronic transition plus a group of neighboring ions participating in the rearrangement. This assembly of an excited particle interacting with neighbors is at times referred to as an exciton. To a first approximation, a single set of potential energy curves are used to describe the ground and excited states of the system. The energy curves are generally parabolic and excited states can be treated as a series of equally spaced vibrational levels. The curves are displaced with respect to each other along the coordinate axis since excitation causes a redistribution of the electronic charge. This caused the atoms to shift to new equilibrium positions which minimize the total energy. Figure 25 shows a typical luminescence process in terms of a configurational coordinate diagram.

In simple luminescence involving only ground and emitting states, absorption consists of an electronic transition directly to the excited state. This occurs while the atomic configuration of the ground state is maintained since the excitation process takes place quickly, before atoms are able to shift to new equilibrium positions. (Frank-Condon principle[29].) Emission occurs, maintaining the atomic configuration of the excited state.

This model clearly emphasizes the rearrangement energy as the origin of the difference in excitation and emission energies. In addition, the model indicates that the atomic configuration, other than the one of lowest energy, has finite probabilities. As a result, all

optical transitions will be broadened and broadening will be temperature dependent. The configuration coordinate model treats each center as independent so that the rates of excitation, rearrangement, and emission depend on the number of centers in the state undergoing the change. Therefore, a monomolecular mechanism should dominate for this analysis to be valid.

Activator systems possess either energy levels which can be identified as free ion states perturbed by crystalline interactions or those which can be better approximated by perturbed states of the crystal band structure. The first type is usually characterized by deep-lying levels frequently below the forbidden gap and emission occurs at the excitation site. These activators are usually excited by inelastic collisions or resonance transfer. The configuration coordinate model is employed to interpret the electroluminescence in these cases. The second type of activator is characterized by a ground state above the top of the valence band and excited states near the conduction band. Excitation of this type of activator may occur by capture of charge carriers or by inelastic collisions. If ionization occurs in a region of high field, carriers are immediately swept from the excitation site. The field must then be removed before conduction electrons are able to return to this region and emission can occur.

b) Mechanisms Responsible for Electroluminescence in ZnS:Mn:Cl

The host lattice in this study was cubic ZnS. Each atom had about it four equally distant atoms of the opposite kind, arranged at the corners of a regular tetrahedron. The band-gap of cubic ZnS has been measured to be 3.7 eV [30].

Since manganese is divalent, it replaces a Zn^{++} ion in the lattice structure. On the other hand, chlorine should be found at interstitial

locations in the lattice as Cl^- because of its diamagnetic character in ZnS. Manganese, present as a substitutional impurity, is responsible for yellow-orange emission in several electroluminescent materials. It was postulated early that manganese luminescence in ZnS:Mn must be due to an electronic transition within the manganese ion [31]. This impurity system possesses deep-lying levels, well below the top of the valence band, which can be approximately described by states of the free divalent ion. Regardless of the ionic or covalent character of the crystal binding in a material, the emission involves states with a $3d^5$ electronic configuration. The stable configuration of a neutral manganese is as follows

$$Mn\ 1s^2\ 2s^2\ 2p^6\ 3s^2\ 3p^6\ 3d^5\ 4s^2.$$

The energy level system for the free manganese ion Mn^{++} possesses the spherically symmetrical ^6S state as the ground state in which all 3d electron spins are parallel [32]. The first excited state may be approximated by the ^4G state which has one spin reversed. Although the quantum numbers L and J lose their meaning in a surrounding which does not have spherical symmetry, they are still used for reasons of convenience of notation.

The resultant change of multiplicity because of spin reversal leads to two results. First, the transitions between the ground state and excited state are forbidden. Second, manganese in the excited state should have a decreased magnetic susceptibility of two Bohr magnetons per atom. The susceptibility is given by

$$X = \frac{J(J+1)g^2B^2}{3\,kT} \qquad (9)$$

where $B = \frac{1e}{2mc}$ (Bohr magneton).

The effective Bohr magneton number is usually expressed by

$$\mu = g\,J(J+1)^{1/2}. \qquad (10)$$

Thus, a change in multiplicity should be detectable experimentally. Johnson and Williams[33] found a change in susceptibility of the order of magnitude predicted. Several perturbations are present in the crystal which cause a mixing of states and a losening of the selection rules. These include the crystalline field, the spin orbit interaction, the exchange coupling of Mn^{++} pairs, and the phonon coupling[31]. The remote possibility of the ionization of the manganese center upon excitation is illustrated in Figure 26. The location of the two lowest energy states of the $3d^5$ electron configuration are shown relative to position of the conduction band in zinc sulfide[1]. It is, therefore, concluded that the yellow emission is a result of transitions within the manganese ion. The energy for transition is provided by either direct collision excitation or the Mn ions by charge carriers or collision excitation of forbidden gap states from which occurs a transfer of energy to Mn atoms.

Configuration coordinates explain the difference between the absorption energy of 3.32 eV and the observed emission energy of 2.1 eV. Figure 27 shows the configuration coordinate analysis for manganese in cubic zinc sulfide. Since the emission was similar to that previously observed in ZnS:Mn, it is clear that the introduction of chlorine into the lattice did not perturb the manganese luminescent center essentially.

The other band of emission was centered at 4500Å. This indicated that it was the same as the blue emission which had been observed in ZnS:Cl. Bowers and Melamed[34] suggested that emission occurred at a

Cl^- site or at a zinc vacancy. Kroger[35] has suggested that a zinc vacancy with one electron missing from an adjacent sulfur is responsible. Zn^+ centers have also been suggested. Koda[36] and Prener and Williams[37] suggest the association of a zinc vacancy and a chlorine ion.

Bowers and Melamed found that the center responsible for blue emission in ZnS:Cl was diamagnetic. Thus, paramagnetic Zn^+ ions can be eliminated as possible luminescent centers. Singly ionized chlorine possesses shallow energy states near the conduction band so that it does not allow for transitions which yield visible radiation. Zinc vacancies are negatively charged sites which would not provide low energy states for the de-excitation of conduction electrons. Thus, none of the proposed mechanisms for the blue emission seemed satisfactory. A new mechanism will, therefore, be proposed which was consistent with the data gathered during this study and that found in the literature.

c) A New Model for E.L. in $ZnS:Mn:Cl_2$

The blue emission band was centered at 4500Å and its intensity increased as the concentration of impurities increased. However, a faint blue emission was also observed in the absence of impurities. The relaxation times for the blue emission were measured to be roughly .02 and .1 m/sec. The brightness of the emission decayed with operating time of the cells, according to Eq. (4). The brightness relation as a function of voltage and frequency was also determined. A new mechanism must be able to explain all these phenomena.

It was a curious fact that blue electroluminescence had been reported in ZnS when any of a variety of impurities had been added, such as Cu^+, Ag^+, Br^-, I^-, and Cl^-. The blue emission was so common that it seemed to be characteristic of the host lattice. As a result,

zinc vacancies had often been proposed as the source of the blue emission in ZnS. Blue emission was also observed when pure zinc sulfide was fired in the presence of atomic sulfur. These observations provided the framework for the formulation of a new model for the blue electroluminescence.

The new model was developed as follows. A common effect of the introduction of $MgCl_2$ into ZnS and the firing of ZnS at high temperatures is the production of Zn^{++} interstitial ions. These ions do not serve as luminescent centers in themselves. However, suppose that a co-activator, such as chlorine, is introduced into the host lattice. Studies of the magnetic properties of ZnS:Cu:Cl have shown that chlorine is present in ZnS as Cl^-. These Cl^- ions are capable of combining with Zn^{++} to form a center of the type $(ZnCl)^+$. Such a center is similar electrically to Cu^+, Ag^+, and Au^+ which possess energy levels in ZnS approximately 2.7 eV below the conduction band. Also, this center is diamagnetic, as has been observed experimentally [34]. Collision excitation of this center ejects the electron shared between the zinc and the chlorine ions into the conduction band and it is swept away by the electric field. When the field is removed, electrons flow back to the region of the center and fall into the potential well created by the doubly ionized $(ZnCl)^{++}$ center, which results in the emission of radiation. The intensity of the radiation depends on the number of luminescent centers which are a function of the impurity concentration. Essentially, it is being proposed that the co-activator chlorine combines with divalent zinc to form an effective activator center of the form $(ZnCl)^+$.

This model does not explain the blue emission which occurred in the absence of any impurities. It was observed that this emission was

enhanced by the introduction of atomic sulfur prior to firing. Introduction of interstitial sulfur could result in the formation of some $S^{=}$ ions. These ions could combine with Zn^{++} ions to produce a center of the type $(ZnS)^{+}$ which would behave in the same manner as the $(ZnCl)^{+}$ center. These centers would be paramagnetic and explain the temperature dependence of the susceptibility of pure zinc sulfide which Bowers and Melamed had observed. Also, they explain the enhancement of the electroluminescence when powders were fired in the presence of atomic sulfur. Most luminescent centers were created under these firing conditions and, thus, the probability of excitation and emission was increased proportionately.

The blue emission was, therefore, attributed to two different centers. In general, the $(ZnCl)^{+}$ centers were much more numerous than the $(ZnS)^{+}$ centers, which was evident from the relative intensities of the electroluminescence in doped and undoped phosphors. The measurements which were made during this work will now be interpreted in terms of the proposed luminescent centers.

d) Correlation of Proposed Model with Observations

To review briefly, it was established that the electroluminescence observed in ZnS:Mn:Cl consisted of two separate bands of emission. One band was centered in the yellow at 5860Å. The other band was centered in the blue at 4500Å. Transitions within the divalent manganese ion were proposed as the mechanism for the yellow emission. Luminescent centers of the form $(ZnS)^{+}$ and $(ZnCl)^{+}$ were proposed as the source of the blue emission. The characteristics of the electroluminescent cells must now be correlated with these proposed models. Injection of carriers from a

conducting electrode into the crystals was not possible so that no external supply of carriers was available. New charge carriers to make up for radiative recombination losses had to be created somewhere within the sample. A certain number of carriers arose with known statistical probability from thermal agitation. Introduction of impurities into a semiconductor increased the probability of electron excitation into the conduction band. In ZnS:Mn:Cl the Cl^- ions yield their extra electron to the conduction band if they are sufficiently excited.

A certain minimum energy is required to produce an excited activator center. A conduction electron which is in an electric field intensity E, acquires the energy which is necessary for excitation of an activator system by an inelastic collision, if it traverses a path L without being scattered. The probability of an electron experiencing a path greater than L is given by the expression

$$P = e^{-L/\lambda} \tag{11}$$

where λ is the mean free path of the electron. The energy acquired from the field over a path L will be

$$\varepsilon = eEL = \frac{1}{2}mv^2 \tag{12}$$

Solving for L

$$L = \frac{mv^2}{2eE} = \frac{\sqrt{2m\varepsilon}}{2eE} \tag{13}$$

The mean free path λ of the electrons in the crystal is the inverse of the frequency of collisions of electrons with lattice phonons.

$$1/\lambda = f \tag{14}$$

Substituting Eqs. (13) and (14) into Eq. (11), the probability of an electron acquiring an energy ε in the presence of a field E is obtained

$$P = \exp - \frac{\sqrt{2m\varepsilon f}}{2eE} \qquad (15)$$

Therefore, with very strong fields, the average conduction electron will acquire energy from the field faster than energy is lost to lattice phonons. It, thus, attains sufficient energies to collision ionize impurities or valence electrons. To obtain electron energies of 2.5 eV, fields on the order of 10^6 v/cm are necessary.

In the presence of the high fields necessary for electroluminescence, the consequences of dielectric breakdown are avoided because of the inhomogeneous field distribution in the crystal. Extremely high fields exist in some regions where breakdown conditions are not approached because of the existence of potential barriers.

The initial application of the field releases electrons from shallow traps into the conduction band. These joined thermal carriers already present. These conduction electrons were accelerated by the applied field. Some carriers achieved energies sufficient to ionize a $(ZnCl)^+$ center or transfer energy to a Mn^{++} center and excite it internally. Thus, both the blue emission and the yellow emission were dependent on charge carrier collisions.

The excitation mechanism described above was consistent with observations made during this study involving constant applied voltages. It was found that d.c. electroluminescence could be observed if electrons were injected into the crystals from one of the electrodes. These injected

carriers were accelerated across the dielectric continuously and a constant light output was observed. If no carrier injection occurred, electroluminescence was only observed upon application and removal of the d.c. voltage. Therefore, accelerated conduction electrons were the mechanism of excitation in $ZnS:Mn:Cl_2$.

In the normal cells in which no direct currents were present, an electric field accelerated carriers to the boundary layer of the crystal. For microcrystals embedded in a dielectric, this boundary was impenetrable. Negative carriers accumulated at the positive boundary and formed a space charge. A corresponding electron deficiency constituted a positive space charge in the remainder of the crystal. Some of the free electrons produced by the applied field were trapped. When the external field was removed, part of the polarization charge decayed quickly in a time similar for build up. That portion of the space charge consisting of electrons in traps decayed very slowly at a rate determined by the thermal release of trapped electrons. This analysis is consistent with the relaxation time measurements, which showed two stages of decay. Acceleration occurred in the volume of the phosphor although potential barriers at the surface influenced carrier motion. The rate of recombination of carriers was governed by the potential distribution of the polarization which had been established by the external applied field. Piper and Williams[38] gave an expression for the electric field intensity due to such a space charge layer.

$$E(x) = -\left(\frac{2\pi enV^{\frac{1}{2}}}{k}\right)(1 - x/d) \qquad (16)$$

where d is thickness of layer

V is applied voltage

n is density of carriers

k is dielectric constant of crystal.

This potential barrier is referred to as a Mott-Schottky[39] exhaustion barrier. The electric field is proportional to the square root of the applied voltage. If trapping or activator levels are present, a field could empty these levels with the probability

$$P = \exp(-\varepsilon/e\mathcal{E}\lambda) \tag{17}$$

where ε is the energy of the level

$\mathcal{E}$ is the electric field intensity

λ is the mean free path.

For this barrier field in particular

$$P = \exp(+\varepsilon/e\beta\sqrt{V}\lambda). \tag{18}$$

This type of probability would agree with the observed brightness relations for ZnS:Mn:Cl which take the form

$$B = B_o \exp(-A/\sqrt{V}) \tag{3}$$

The constant A would then be linked with the depth of the trapping levels which were evacuated by the field and the activation energies necessary to excite the luminescent centers. The larger value of A obtained for the manganese emission energy of 2.1 eV versus 2.7 eV for the $(ZnCl)^+$ center.

Although the manganese centers did not provide any of the conduction electrons which made up the space charge layer, they were dependent on these

accelerated charges for excitation by collisions in the same manner as the blue centers. Therefore, it was not surprising that both emission bands possessed the same type of brightness versus voltage characteristics.

The frequency dependence of the emissions was explained by similar analysis. The brightness increased linearly with frequency at low frequencies since conduction electrons were making more traversals of the crystals and, therefore, exciting luminescent centers more frequently. Eventually, saturation of brightness occurred when the relaxation times of the luminescent processes became longer than the period of the applied field.

Also, brightness waves were interpreted by means of this model. For each cycle of the applied field, donor ionization, electron acceleration, and excitation of centers began anew. The maximum peak occurred when the polarization field and external field, which had just reversed, supported one another. Yellow emission occurred before blue because its relaxation time is smaller. Physically, this was reasonable since the manganese center did not require the return of carriers from other regions of the crystal in order to undergo de-excitation.

We can summarize this treatment as follows. It was proposed that a space charge was built up at the opposite surfaces of a crystal. This build up resulted in the establishment of a Mott-Schottky potential barrier whose electric field was proportional to the square root of the applied voltage. Electrons which had fallen into traps were released when the external field was removed. Carriers were accelerated through the bulk of the crystal. Electroluminescence only resulted in regions where carrier density and electric fields were sufficiently high. This explanation was in accord with the experimental measurements of brightness, brightness waves, and relaxation time made during this study.

The aging of the electroluminescent cells was a difficult phenomenon to explain. The brightness of the cells was observed to deteriorate as expressed by Eq. (4)

$$B = B_0 \frac{1}{1 + t/\tau_{1/2}} \qquad (4)$$

It was observed that $\tau_{1/2}$ was a function of the applied frequency and impurity concentration. Figure 28 shows the fit of experimental data to an equation of the above form for over 200 hours of test on a typical cell.

The consensus of the work done by others was that the aging took place due to purely physical processes within the phosphor grain itself (40) Roberts had ruled out a change of dielectric constant and conductivity of the supporting dielectric as the cause of decay. Effects of moisture were dismissed because cells were sealed. The electrical characteristics of the cells remained essentially unchanged which tended to support these assumptions. Care was taken to avoid use of cells which showed any signs of sparking or breakdown. Thus, it was assumed that any decay in electroluminescence should be interpreted as changes in the phosphor. An attempt was made to correlate the decay of the brightness in ZnS:Mn:Cl to the luminescent centers that had been proposed.

Consider the general form of a second-order rate equation involving the concentrations of two types of substances A and B (41). Here A represents $(ZnCl)^+$ centers and B represents Cl^- ions.

$$\frac{dA}{dt} = \frac{dB}{dt} = k\,(A)\,(B) \qquad (19)$$

Suppose n_o and m_o are initial concentrations of A and B and let x be the decrease in concentration of A and B for the reaction A + B = products. Then

$$dx/dt = k(n_o - x)\ (m_o - x) \tag{20}$$

If m and n are equal

$$t = \frac{1}{1/k\ (n_o - x)} - \frac{1}{kn_o} \tag{21}$$

Now if electroluminescent emission is directly related to the number of emission centers n where

$$n = n_o - x \tag{22}$$

Substituting (22) in (21)

$$t = 1/kn - 1/kn_o \tag{23}$$

Solving for the number of emission centers n at any time t

$$n = \frac{n_o}{1 + kn_o t} \tag{24}$$

This result was interesting since the predicted decrease in the number of luminescent centers with time was of the same form as the observed brightness deterioration provided that the following equality was assumed

$$kn_o = 1/\tau_{1/2} \tag{25}$$

The half life of decay was, therefore, a function of the concentration of the luminescent centers and the rate constant. It was consistent with measurements which indicated an increase in 1/2 with

increased operating time. This was attributed to a decrease in the number of luminescent centers in accordance with Eq. (25).

If for every $(ZnCl)^+$ luminescent center there was a free Cl^- ion diffusing through the lattice, the above equations would govern the recombination of these ions. $(ZnCl)^+$ and Cl^- would combine to produce stable $ZnCl_2$. This would be an irreversible process and would result in the reduction of the number of luminescent centers at a rate predicted by Eq. (24). Mn^{++} should be the dominant factor in the production of Zn^{++} vacancies. There are two Cl^- ions for each Mn^{++} ion. Thus, half of the Cl^- ions could combine with zinc vacancies while the other half could be free to diffuse through the lattice. The rate of diffusion of the chlorine ion would determine the rate of decay for the proposed mechanism. Jaffe (42) had studied the deterioration of electroluminescence of ZnS which was doped with either chlorine, bromine, or iodine. If the diffusion of the halide ion was involved, the rate of decay of these phosphors should differ. Since the heavier halides were less mobile, these should have decayed at a slower rate. This hypothesis was borne out of Jaffe's results. ZnS:Cl decayed more rapidly than ZnS:Br or ZnS:I. The mobility of these halides definitely appeared to be linked to the decay of brightness with operating time.

Therefore, a conclusion of this study was that the decay of the electroluminescent blue emission in ZnS:Mn:Cl was the result of the annihilation of $(ZnCl)^+$ luminescent centers by means of diffusing Cl^- ions.

However, the yellow manganese emission was also observed to decay with time. This need not be explained in terms of the reduction of manganese centers. Manganese ions were dependant on accelerated charge

carriers for excitation by inelastic collisions. For each $(ZnCl)^+$ luminescent center which was annihilated, a potential electron carrier was lost. Thus, fewer electrons were available for ionization into the conduction band as time increased. Fewer carriers resulted in a reduction in the probability of manganese excitation. The slower rate of decay observed in manganese was attributed to several factors. The number of Mn^{++} luminescent centers remained relatively stable whereas the $(ZnCl)^+$ centers were reduced in number. Also, the yellow emission (2.1 eV) was of lower energy than the blue emission (2.7 eV) so that a greater percentage of electrons were capable of exciting the yellow emission and a loss of carriers was not so critical.

Another aspect of the aging to be explained was the strong dependence on the frequency of the applied field but little dependence on the amplitude. This phenomenon had never been satisfactorily explained although similar frequency effects had been observed [43]. An analysis of the problem was attempted.

It was assumed that the diffusion of Cl^- ions was responsible for the observed decay in brightness. Decay occurred only during operation of the cells so that thermally induced diffusion of chlorine at room temperature was not responsible for the decay. Since decay was observed during cell operation, some authors [44] have concluded that field enhanced diffusion of ions was responsible for the decay. This was possibly the mechanism for the observed decay of d.c. electroluminescence in which an ion would feel a constantly applied force in the same direction. However, in an a.c. field, the average of electrical forces exerted by the field on the ion cancels. Also, since studies made here failed to detect any influence on the strength of the

applied field on the decay rate, the conclusion was reached that the force qE exerted on the ion was not responsible for the observed deterioration under a.c. conditions.

It was observed that at low frequencies of operation (below 250 cps) the brightness remained essentially constant in time. As the frequency of operation was increased, the rate of decay increased. It was difficult to explain how the applied frequency could so drastically effect the decay rate. There was the possibility that it was not the applied frequency in itself which was the source of the deterioration but rather some frequency dependent parameter. The input power to an electroluminescent cell increased quite rapidly as the frequency was increased (Figure 23). Also the efficiency of the cells was greatly reduced at high frequencies so that a greater percentage of the energy was absorbed by non-radiative processes such as lattice vibrations. Studies made here showed that even the best cells were only about two per cent efficient. The electroluminescence was confined to very small regions of the phosphor. As a result, local temperatures in the region of these high fields and currents were much higher than the average temperature of the cell. Cells which were operated at high frequencies over long periods became hot to the touch so that local temperatures could be quite high.

This cell behavior suggested the thermally induced diffusion of Cl^- ions rather than the field assisted diffusion which had been proposed in the literature. Thermal diffusion of chlorine should obey Fick's law given in Chapter I.

$$J_o = D \exp - H/kT \operatorname{grad} N \qquad (1)$$

At low frequencies the input power was so small that the temperature of the phosphor dielectric layer was not sufficient to affect the diffusion of ions. Thus, no decay was observed. As the frequency was increased the input power increased so that local temperatures rose and stimulated the diffusion of Cl^- ions.

Such a hypothesis was also consistent with the observed decay of cells with different amounts of dopant material. At higher concentrations of impurities, the likelihood of nearby Cl^- ions was increased so that the term grad N in Eq. (1) was decreased. The diffusion rate of the impurities would be slowed and, therefore, the decay of brightness. This was exactly the behavior that was observed in the cells. The more highly doped powders decayed at a slower rate. At the same time these highly doped powders had a greater light output.

This analysis also explains why the dielectric material, in which the phosphor was suspended, influenced the rate of decay [45]. The aging rate will depend on the ratio of the energy dissipated in the dielectric to the energy dissipated in the phosphor. Thus, it would be expected that the choice of the dielectric layer would affect the rate of decay since it influences the energy distribution between it and the phosphor.

Thus, thermally induced diffusion of the Cl^- ion to $(ZnCl)^+$ centers was proposed as the mechanism responsible for the decay of brightness with time in ZnS:Mn:Cl. This mechanism was in accord with the experimental evidence which was gathered during this study and which had been reported in the literature.

A brief summary of the relaxation time studies will now be given. It was observed that all cells emitted light on the application and removal of a d.c. voltage. The latter emission was always larger than the

initial pulse. This was easily explained in terms of the Mott-Schottky barrier discussed earlier. When the field was applied the internal polarization field opposed the external field so that carrier acceleration was reduced. However, when the external field was removed the polarization field was unopposed so that greater energies were attained by carriers. Thus, more luminescent centers are excited.

The emission which occurred upon the removal of the external field took the form of a double exponential decay with one process occurring more rapidly than the other. The field-assisted release of carriers from traps near the conduction band explained this two stage decay.

Conduction band electrons in the space charge layer were immediately released when the external field was removed and were characterized by relaxation time τ_1 in Eq. (5). The release of trapped electrons dominated the second stage of the output with relaxation time τ_2. The measured values of τ_1 and τ_2 were weighted averages of emission from thousands of microcrystals of varying sizes, electric field intensities, and carrier concentrations. Since the electric field of the space charge layer in each individual microcrystal was the determining factor for the relaxation time, this made it impossible to interpret the average relaxation times in terms of specific trapping levels. Also, there is evidence (46) that the alignment of the crystalline axes, with respect to the applied field, was important in electroluminescence due to anisotropy of ZnS. In these powder cells random alignment was present which served to further complicate matters. It seemed that single crystals, rather than crystalline powders, were necessary to obtain accurate relaxation times since problems due to crystalline alignment and averaging would be eliminated. However,

the measurement of the relaxation times of these powder cells did serve a useful purpose since it supplied further evidence for the model of electroluminescence that had been proposed. For example, the saturation of cell brightness with increasing applied frequency was consistent with the relaxation time measurements. The distribution of the yellow and blue emission in the brightness waves was explained by the results of the different relaxation times which had been found for each emission. Also, possible trapping of conduction band electrons was suggested by the measurement of the average relaxation times.

Chapter IV - Magnetic Properties of ZnS:Mn:Cl_2

a) Some General Considerations

In spite of the large amount of work already done in connection with ZnS phosphors, it still remains a partially puzzling problem. It might well be that the reason for this situation is determined by the fact that for E.L. to take place rather complicated situations have to exist. In order to get a handle on this kind of a situation, it becomes necessary at times to solve only a small part of the whole problem. Electrically E.L. cells are lossy capacitors and optically they are broad band emitters. Neither aspect is apt to yield a great deal of detailed information about the electron kinetics of the process. Clearly, since the emission occurs in the visible part of the spectrum the involved transitions must be at least in part electronic in nature. One obvious way of monitoring the electrons consists in observing the magnetic behavior of the cells, both in the absence and presence of an electric field. Although a great deal of EPR work has been done in this connection, we are not aware that anybody ever used electrical excitation for these observations. The usual procedure consists in pumping electrons optically from, or into, localized sites and deduce from the change in the observed EPR signal such information as, for example, trapping depths or life times.

We decided, therefore, to attempt obtaining signals during the state of electroluminescence. Some care is necessary to avoid obvious pitfalls. First of all, the signal obtained from an EPR bridge is proportional to the loaded Q of the cavity. Hence, it was mandatory to make samples (Chapter I) which did not penetrate much into those regions of the cavity

where there is a strong r.f. electric field. Since dielectrics - in this case, the matrix in which the phosphor powders were embedded - are usually quite lossy, it was decided to perform the experiment with a thin lossy sample located along the axis of a cylindrical cavity. Electrical connections could then be made outside of the cavity proper. A first attempt to obtain changes in the EPR signal with phosphors made from the above-mentioned Sylvania powders failed. It was difficult to ascertain that the samples actually emitted light because phosphors made from pure powders exhibit very little brightness and since the sample was completely enclosed in a thin gold layer, with resulting loss of transmitted power, the results remained inconclusive. We, therefore, repeated the experiment with a powder obtained from the Fisher Company, which is known to have a larger content of initial impurities, in particular - copper. In the following we report exclusively on cells made with the latter powders.

b) EPR Bridge Measurements and Experimental Procedures

All EPR measurements were done with an X-band spectrometer (Strand Lab-Model 602). Figure 29 is a schematic diagram of the equipment. Its essential features are the following. A klystron, separated from the rest of the system by a Ferrite isolator, feeds power to a directional coupler. There the power is partially led to a balanced mixer and in part through a wave meter (reference cavity) to the second input of the mixer. Any change in the klystron frequency is sensed, the resultant signal converted into a voltage which is applied to the repeller of the klystron to force its frequency back to that of the reference cavity. In this manner, the klystron is "locked" to the wave meter. When this procedure is followed, one measures the real part of the susceptibility

(dispersion mode). For the work done under this contract, it turned out to be more convenient to measure the imaginary part of the susceptibility (absorption mode). In this case, the reference cavity is merely used to measure the frequency while the klystron is locked to the sample cavity. This is done by dividing the power from the klystron into two parts - one being sent into the reference arm of the bridge to another balanced mixer while the other proceeds to a circulator where it is split again, one part going directly to the second input of the balanced mixer, the other part first being reflected by the sample cavity. The output of the balanced mixer is again converted into a voltage which when applied to the repeller of the klystron locks it to the sample cavity. A second set of crystals in the mixer is used as a detector, its output being fed through an amplifier to a phase detector. The second input to the phase detector comes from a 6 Kcps oscillator, which also activates the modulation coils on the magnet. The measurements are made by balancing the bridge, i.e., by arranging to have the power reflected from the cavity just cancel the power which merely passes by the circulator. As the magnetic field of the magnet is swept through the resonance field of the sample to be examined, power will be absorbed, the bridge unbalanced, and a signal detected. What is finally recorded is the derivative of the absorption signal.

Figure 29a is a schematic - not drawn to scale - showing the arrangement of the wire in the cavity. The two teflon caps are essential in preventing the wire from moving in the cavity while the experiment is in progress.

c) Results Obtained With $ZnS:MnCl_2:10^{21}$

Since Mn^{++} does not only have a $^6S_{5/2}$ electronic ground state but also five nuclear spins, one would expect a total of thirty lines.

In our case, the observation being made at 300°K and with polycrystals, only six broad lines are observed corresponding to the selection rules $\Delta M_n = 0$. If, in addition, the concentration of the Mn^{++} impurity is so high that there is broadening due to spin coupling of neighboring Mn^{++} ions, only one line is observed. Figures 30 demonstrate the change in the observed spectrum as a function of impurity concentration. Figure 31 presents the spectrum for 10^{21} Mn^{++} ions per cm^3 with, and without, applied E.L. field. In order to evaluate this result in terms of changes in absorbed power, it is necessary to make an assumption concerning the shape of the absorption line which is taken to be Lorentzian. Then the total light of the derivative curve is proportional to the absorbed power. Table 5 presents the relative changes in absorption for a variety of frequencies and voltages applied to the sample. The values presented were obtained by assuming a Lorentzian line shape.

TABLE V

RELATIVE MICROWAVE ABSORPTION FOR $ZnS:MnCl_2:10^{21}$

V (volts)/f (Kcps)	5	10	15	20	25
800	.98	.96	.91	.89	.89
900	.97	.93	.87	.85	.85
1000	.96	.89	.85	.80	.82
1100	.94	.87	.82	.77	.80

All values quoted are accurate within ± .02. First of all, it is apparent that the values do not change any longer beyond 20 Kcps. We attribute this to a relaxation process taking place with a characteristic time of about 45 microseconds. Next, one notices that within the quoted experimental error, the signal with applied voltage S_v divided by the signal without

applied voltage S_o behaves as

$$\frac{S_V}{S_o} = r = 1 - afV^3 \,. \qquad (26)$$

This is an experimentally derived relationship and was arrived at in the following way. Figure 32 presents r as a function of applied frequency for the various voltages. A least square approximation yields straight lines for $r = r(f)$:

$$r = 1 - c\,f \qquad (26a)$$

where f is the applied frequency and c has the following values for the various voltages:

V	800	900	1000	1100
C	.0054	.0077	.010	.012

A further evaluation of the slopes finally leads to the conclusion that the constant c is proportional to V resulting in Eq. (26) with "a" having a value of $(1.0 \pm .1) \times 10^{-14}$ sec V^{-3}. The values actually obtained for a are as follows:

V	800	900	1000	1100
a	1.11×10^{-14}	1.06×10^{-14}	1.00×10^{-14}	$.95\times10^{-14}$

The fact that "a" changes in a rather regular manner is undoubtedly of importance but so far we have not been able to explain this effect completely. We believe, however, that one can safely assume that Eq. (26) is not strictly true, since possible changes in the reflectivity of the sample with applied voltage have not been taken into account. In order to ascertain that the changes in the observed signal are not all due to changes in the reflectivity of the samples a sandwich type sample, as

used for the optical measurements, was used to reflect a beam of 10 KMc microwave power. Since no change in the reflectivity was observed - the sensitivity of the equipment not being sufficient to observe changes as expressed by the small variations in a - as a voltage was applied to the sample, we take this as a justification of our interpretation.

d) Results for Smaller Concentrations

Attempts to obtain similar results for a concentration of 10^{18} impurities per cm^3 did not yield any positive results at all. The results for 10^{19} and 10^{20} $MnCl_2$ per cm^3 are presented in Tables 6 and 7. The evaluation of these data is quite complicated since what is essentially observed is the "superposition" of two absorption spectra. One is the broad banded line due to spin-spin coupling of Mn^{++} ions and the other consists of the six separated lines of a single Mn^{++} ion. Since both of them change whenever the sample is excited with an applied voltage and neither change is known, it is not at all clear what procedure for the evaluation should be followed. Another way of stating this problem is to say that six individual lines are no longer Lorentzian and, therefore, cannot be evaluated as was done for the case of stronger doping. However, it was hoped that possibly some information might be obtained by considering the average absorption of all six lines. When this is done one obtains

$$r = 1 - KfV^3$$

with K taking on the following values for the different voltages

V	1000	1100	1170	1250
K	9×10^{-15}	8.3×10^{-15}	8.8×10^{-15}	7.7×10^{-15}

TABLE VI

RELATIVE MICROWAVE ABSORPTION FOR $ZnS:MnCl_2:10^{20}$

V	F	1	2	3	4	5	6	V	F	1	2	3	4	5	6
1000	5	.98	.94	.94	.98	.94	.97	1000	20	.84	.75	.76	.78	.81	.80
1100	5	.99	.94	.95	1.07	.91	.95	1100	20	.78	.72	.74	.75	.73	.74
1170	5	.96	.95	.95	1.00	.94	.94	1170	20	.80	.71	.74	.73	.74	.74
1250	5	.94	.91	.89	.99	.96	.93	1250	20	.76	.70	.68	.74	.77	.71
1000	10	.96	.92	.93	.90	.92	1.00	1000	25	.77	.77	.78	.80	.80	.76
1100	10	.91	.92	.92	.87	.92	.94	1100	25	.78	.74	.71	.72	.77	.75
1170	10	.87	.90	.86	.89	.91	.87	1170	25	.80	.72	.71	.77	.75	.71
1250	10	.82	.82	.84	.79	.80	.85	1200	25	.76	.72	.71	.72	.73	.71
1000	15	.86	.86	.86	.88	.84	.86								
1100	15	.81	.82	.77	.89	.82	.78								
1170	15	.76	.77	.74	.79	.78	.74								
1200	15	.79	.76	.72	.76	.73	.74								

AVERAGE VALUES FOR ALL 6 LINES

F/V	1000	1100	1170	1250
5	.96	.97	.96	.94
10	.94	.91	.88	.82
15	.86	.82	.76	.75
20	.79	.74	.74	.73
25	.78	.74	.74	.73

TABLE VII

RELATIVE MICROWAVE ABSORPTION FOR $ZnS:MnCl_2:10^{19}$

V	F	1	2	3	4	5	6	V	F	1	2	3	4	5	6
800	5	.96	1.00	.95	.96	.94	1.05	800	20	.99	.93	.99	.95	1.02	.94
900	5	.94	.98	.91	.96	.93	1.01	900	20	.93	.92	.96	.98	1.06	.93
1000	5	.93	.99	.93	.95	.92	1.01	1000	20	.94	.93	.91	.98	.97	.98
1100	5	.91	.96	.91	.95	.93	.98	1100	20	.95	.90	.96	.96	.99	.96
800	10	1.03	1.03	1.06	.97	.98	1.00	800	25	.95	.97	1.01	.97	.97	.95
900	10	.99	.97	1.04	.97	.94	1.07	900	25	.97	.95	1.01	.96	.96	.96
1000	10	.96	.94	1.03	.94	.97	.94	1000	25	.93	.94	.96	.95	.95	.85
1100	10	1.01	.97	1.00	.90	.96	.98	1100	25	.91	.89	.98	.96	.98	.93
800	15	.94	.99	1.12	.98	.96	1.03								
900	15	.97	.98	1.06	.97	.92	.94								
1000	15	.94	.95	1.02	.96	.91	.94								
1100	15	.91	.95	1.02	.94	.94	.93								

AVERAGE VALUES FOR ALL 6 LINES

F/V	800	900	1000	1100
5	.98	.96	.96	.94
10	1.01	1.06	.96	.97
15	1.00	.97	.95	.96
20	.97	.96	.94	.95
25	.97	.97	.95	.94

From this result it is clear that this approach is too crude to yield any details. However, it is significant that the constant K occurring here is somewhat smaller than that of the case of 10^{21} impurities per cm^3. Any further reduction of the impurity content should make the evaluation worse unless a different approach can be worked out. This is done at present but unique and definite results have not as yet been obtained. In particular, we believe that those values that are larger than unity in Table 7 are not real but are due to our rough evaluation.

Returning briefly to Table 6, an equation of the type (26) was applied to each individual line and the following numbers for the constant K (10^{15}) obtained for the various voltages:

	V	1000	1100	1170	1250
Line 1		.72	.60	.75	.72
Line 2		1.0	.75	.81	.82
Line 3		1.0	.9	.88	.87
Line 4		.90	.61	.75	.72
Line 5		.90	.90	.81	.77
Line 6		.74	.90	.88	.77

It is seen clearly that only for Line 3 is it possible to observe a trend. This is probably due to the fact that this line is closest to the top of the broad spin-spin coupling line.

e) Discussion of Results and Conclusions

Reviewing and summarizing the EPR data yields the following:

1. No changes of EPR signals are observed with $ZnS:MnCl_2$ when the starting product is pure ZnS.

2. Changes are observed when the ZnS powders contain copper impurities and the concentration is at least 10^{19} Mn^{++} per cm^3.

3. As far as the data could be evaluated in a sensible fashion, the ratio of the EPR signals with, and without, voltage is given by the equation

$$r = 1 - af V^3$$

We interpret these results as follows. As a voltage is applied to the samples some Mn^{++} are excited, others are ionized. The first excited state of Mn^{++} is a ^4G state in the free ion approximation. Since we did not observe any change in the EPR signal for pure ZnS powders, this may be attributed to a very fast relaxation time from the ^4G to the ^6S ground state. On the other hand, we did observe changes in the signal when copper was present. We conclude that the Mn^{++} ions are partially ionized and the Cu^+ levels act as traps.

Of major importance, furthermore, is the fact that the changes in the ground state population, or the relative values of the EPR signal, depend on the third power of the applied voltage. We interpret this result as follows. As a voltage is applied to the sample, electrons in the conduction band are accelerated. They interact with the lattice, thereby creating phonons (heat). Only after this preliminary process has taken place are conduction electrons then able to excite or ionize Mn^{++} particles. Since the heating effect goes as V^2 and the cross section for ionization and/or excitation for Mn^{++} may be assumed to be proportional to the energy of the conduction electrons, one obtains a V^3 dependence of the pumping of the ^6S level of Mn^{++}. This interpretation of the EPR data is in full agreement with the results obtained from the efficiency measurements which often yield results of 2% or less efficiency.

It appears, therefore, that electroluminescence takes place only after the greater part of the power put into the sample has been dissipated in the form of heat.

PART II

Electro-Optic Effect

Preliminary measurements established the feasibility of controlling the equilibrium temperature of a metallic surface by adjusting the magnitude of the electric field intensity using polarization techniques. Ordinary polaroids were used and measurements were made of the equilibrium temperature with the polaroids crossed and uncrossed. A change in the equilibrium temperature of the order of 47°K was noted. Since it is obviously undesirable to require mechanical orientation of the polaroids to effect control of the light intensity incident on the metal surface, an electro-optic cell was introduced between two crossed polaroids and the intensity of the transmitted light was measured as a function of the d.c. bias field applied to the electro-optic crystal. In the range from 0V d.c. bias to 9000V d.c. bias, the light intensity increased by a factor of three. Though these results were interesting, the enormous practical difficulty of implementing such a technique over large surfaces did not warrant further efforts in this area.

LIST OF REFERENCES

1. Piper, W. W. and Williams, F. E. Solid State Physics 6. Academic Press, New York. 1958.

2. Gudden, B. and Pohl, R. W. Enhancement of Phosphorescence by Electric Fields. Zeitshrift der Physik 2, 192. 1920.

3. Destriau, G. Experimental Studies on the Action of an Electric Field on Phosphorescent Sulfides. J. de Chimie Physique 33, 620. 1936.

4. Kittel, C. Introduction to Solid State Physics. Second Edition. John Wiley and Sons, Inc., New York. 1956.

5. Lehmann, W. Contact Electroluminescence. J. Electrochem. Soc. 104, 45. 1957.

6. Wachtel, A. ZnS:Cu,Cl and (Zn,Od)S:Cu,Cl Electroluminescent Phosphors. J. Electrochem. Soc. 107, 602. 1960.

7. Shrader, R. E. and Larach, S. Effects of Temperance on the Spectral Distribution of Blue Emission Bands of ZnS:I and ZnS:Cu,I Phosphors. Phys. Rev. 103, 1899. 1956.

8. Curie, D. Luminescence in Crystals. John Wiley and Sons, Inc. New York. 1963.

9. Siddull, G. The Preparation of Electroluminescent Panels, Vacuum VII. 61. 1957.

10. Roberts, S. Ageing Characteristics of Electroluminescent Powders J. Appl. Phys. 28, 262. 1957.

11. Alfred, G. F. and Taylor, J. B. Electroluminescence in Single Crystals of ZnS. Proc. Phys. Soc. London B. 66, 775. 1955.

12. Zalm, P., Diemer, G. and Klasens, H. A. Some Aspects of the Voltage and Frequency Dependence of Electroluminescent ZnS. Phil. Res. Reports 10, 205. 1955.

13. Alfrey, G. F. and Taylor, J. B. Electroluminescence in Single Crystals of Zinc Sulfide. Proc. Phys. Soc. London B. 68, 775. 1955.

14. Piper, W. W. and Williams F. E. The Mechanisms of Electroluminescence in Zinc Sulfide. Brit. J. Appl. Phys. 6, 539. 1955.

15. Zalm, P., Diemer, G. and Klasens, H. S. loc. cit.

16. Waymouth, J. F. and Bitter, F. Experiments on Electroluminescence. Phys. Rev. 95, 941. 1954.

17. Jaffe, P. M. On the Theory of Electroluminescence Deterioration. J. Electrochem. Soc. 108, 711. 1961.

18. Roberts, S. Ageing Characteristics of Electroluminescent Phosphors. J. Appl. Phys. 28, 267. 1957.

19. Henish, H. K. Electroluminescence. The Macmillan Co., New York. 1962.

20. Zallen, R., Erikson, W. T. and Alburg, H. Electroluminescence under Pulsed Square Wave Excitation. J. Electrochem. Soc. 107, 288. 1960.

21. Gillson, J. L. and Darnell, F. J. Electroluminescence in Zinc Sulfide. Phys. Rev. 125, 149. 1962.

22. Fisher, A. G. Electroluminescent Lines in ZnS Powder Particles, Part I. J. Electrochem. Soc. 109, 1043. 1962.

23. Thorton, W. A. Electroluminescence Deterioration. J. Appl. Phys. 28, 313. 1957.

24. Damaskova, S. Time-dependence of Electroluminescence of ZnS:Cu,Mn. Czeck. J. Phys. 9, 529. 1959.

25. Alexander, E. and Steinberger, I. T. Electroluminescence Emission Spectra of ZnS Single Crystals. J. Electrochem. Soc. 109, 870. 1962.

26. Thorton, W. A. Electroluminescence in ZnS. Phys. Rev. 102, 38. 1956.

27. Williams, F. E. Review of the Interpretations of Luminescence Phenomena. J. Opt. Soc. Amer. 39, 648. 1949.

28. Klick, C. C. and Schulman, J. H. Luminescence in Solids. Solid State Physics 5. Academic Press, New York. 1957.

29. Condon, E. V. and Shortley, G. H. The Theory of Atomic Spectra. Cambridge, University Press, England.

30. Czyzak, S., Reynolds, D., Allen, R. and Reynolds, C. On the Properties of Single Cubic Zinc Sulfide Crystals. J. Opt. Soc. Amer. 44, 864. 1954.

31. Langer, D. and Ibuki, S. Zero Phonon Lines and Phonon Coupling in ZnS:Mn. Phys. Rev. 138A, 880. 1965.

32. Klick, C. C. and Schulman, J. H. On the Luminescence of Divalent Manganese in Solids. J. Opt. Soc. Amer. 42, 910. 1952.

33. Johnson, P. D. and Williams, F. E. Some Magnetic Properties of Manganese Activated Luminescent Solids. J. Chem. Phys. 17, 435. 1949.

34. Bowers, R. and Melamed, N. T. Luminescent Centers in ZnS:Cu,Cl Phosphors. Phys. Rev. 99, 1781. 1955.

35. Kroger, F. A. and Vink, H. J. Origin of Florescence in Self-Activated ZnS, CdS and ZnO. J. Chem. Phys. 22, 250. 1954.

36. Koda, T. and Shionoya, S. Nature of Self-Activated Blue Luminescence Center in Cubic ZnS:Cl Single Crystals. Phys. Rev. 136A, 541. 1964.

37. Prener, J. S. and Williams, F. E. Associated Donor-Acceptor Luminescent Centers. Phys. Rev. 101, 1427. 1956.

38. Piper, W. W. and Williams, F. E. loc. cit.

39. Shockley, W. Electrons and Holes in Semiconductors. Van Nostrand, New York. 1950.

40. Roberts, S. loc. cit.

41. Rogers, L. Kinetics of Electroluminescent Deterioration in Some ZnS Phosphors. J. Electrochem. Soc. 111, 411. 1964.

42. Jaffe, P. M. On the Theory of Electroluminescence Deterioration. J. Electrochem. Soc. 108, 711. 1961.

43. Thorton, W. A. loc. cit.

44. Jaffe, P., Roberts, S. loc. cit.

45. Henish, H. loc. cit. 268.

46. Strock, P. Electroluminescence. Electronics World. Jan. 1965.

Figure 1

Basic Construction of Electroluminescent Cell

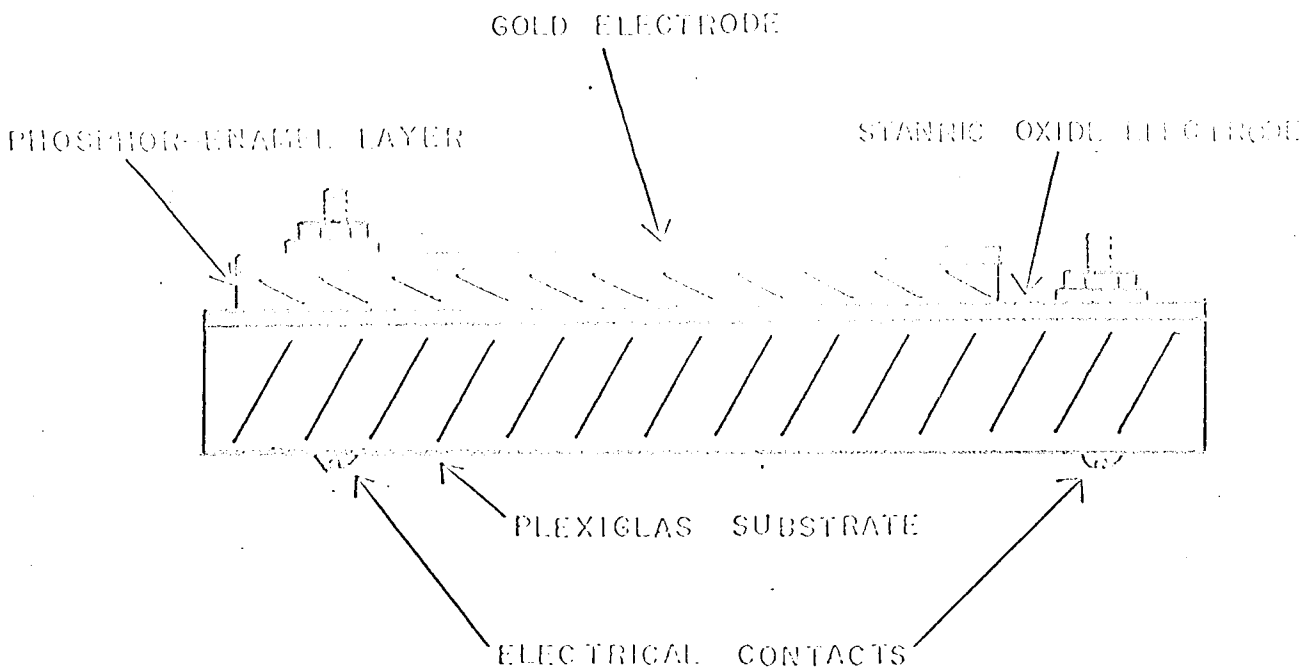

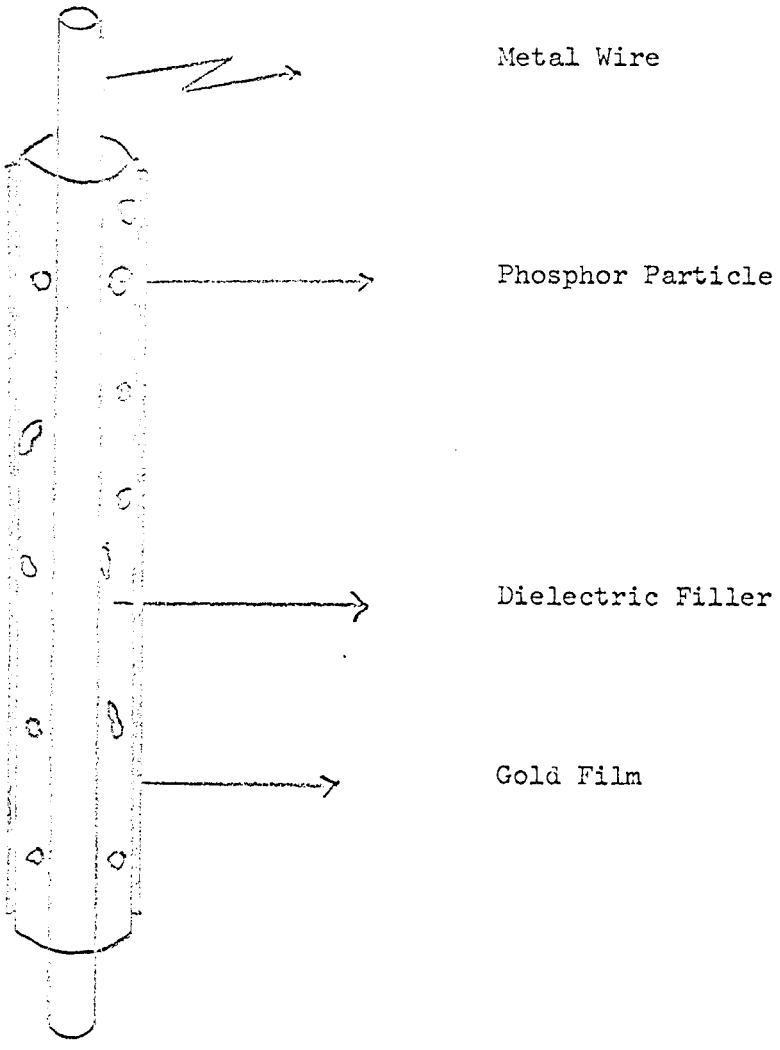

Schematic of EPR Sample

Figure 1a

Figure 2

Block Diagram of Apparatus for Spectral Emission Measurements

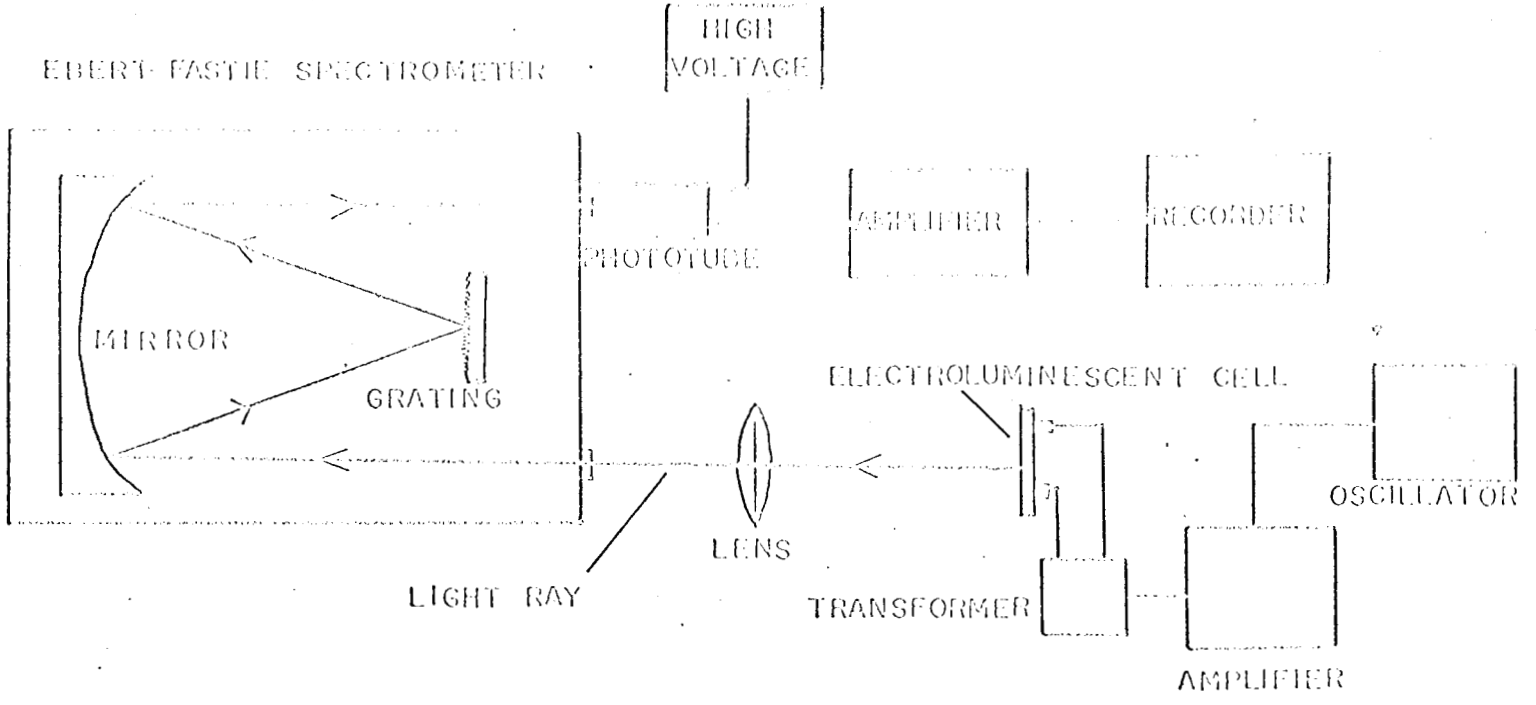

Figure 3

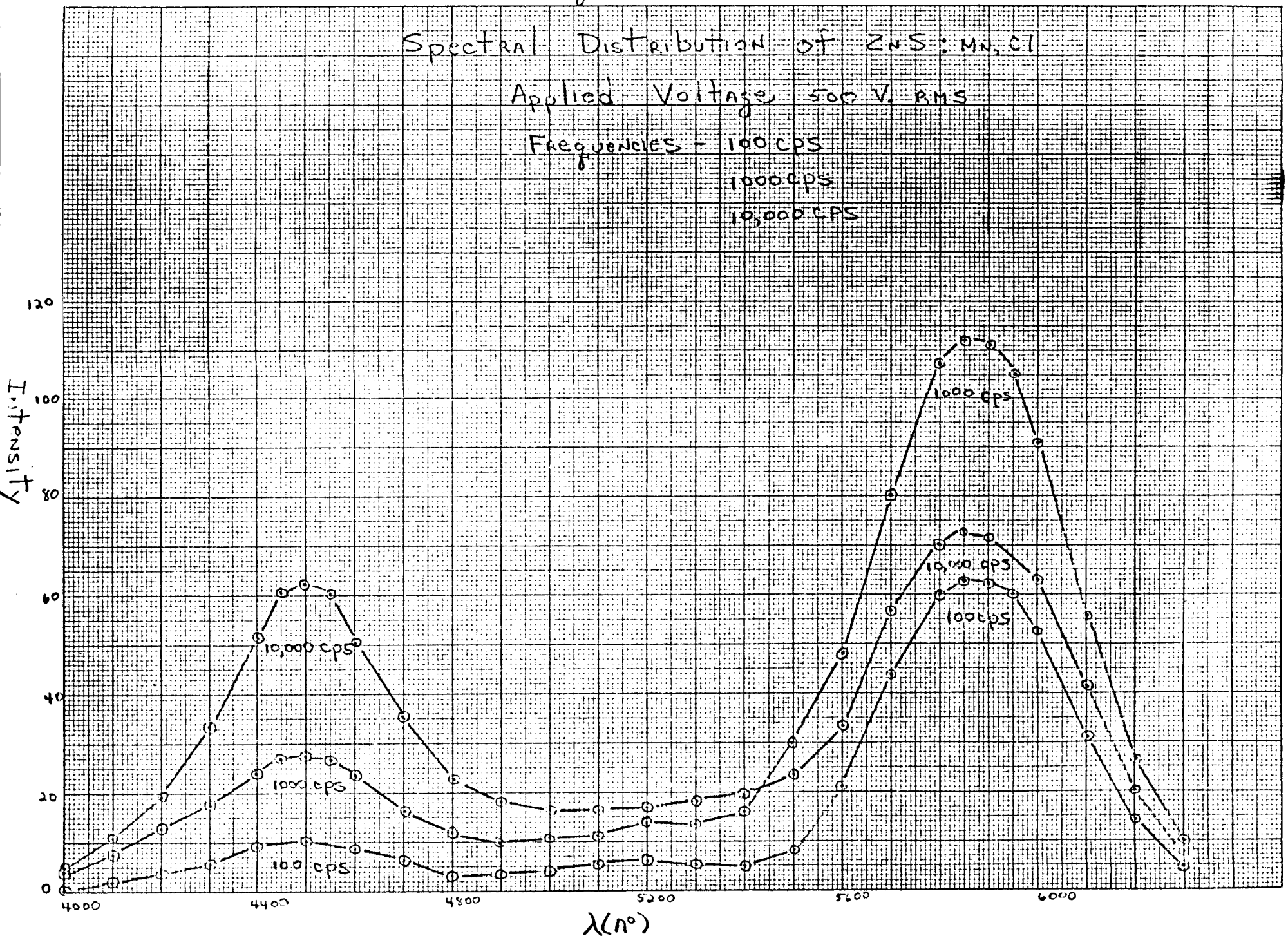

Figure 4

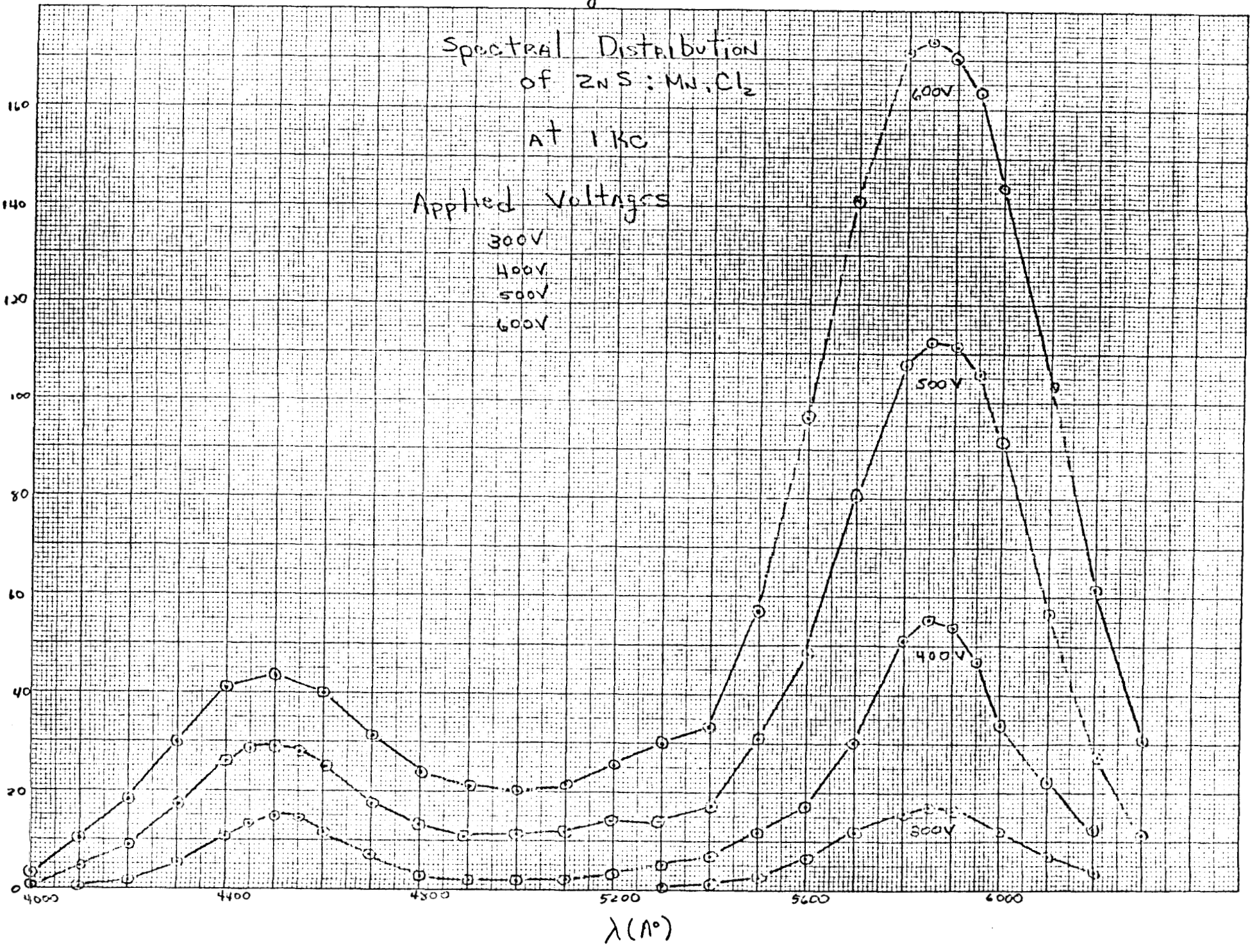

Figure 5

Filter Transmission vs. Wavelength

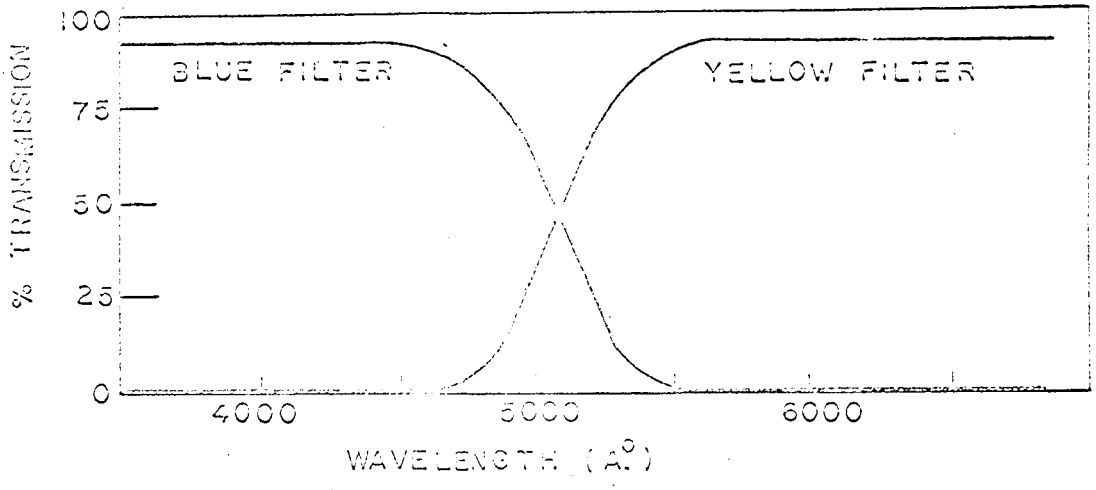

Figure 6

Block Diagram of Apparatus for Brightness Measurements

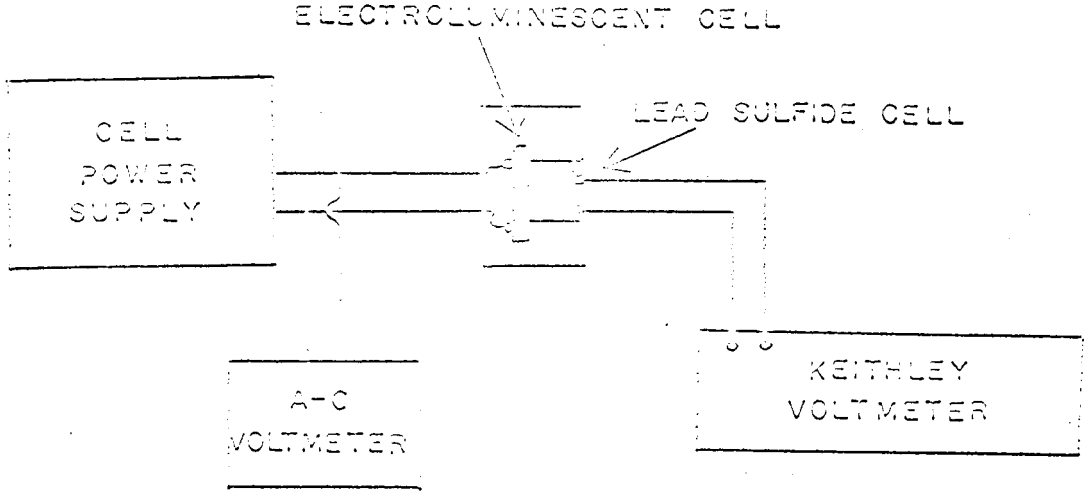

Figure 7

Brightness vs. Inverse Square Root of Applied Voltage for Yellow Band of ZnS:Mn,Cl

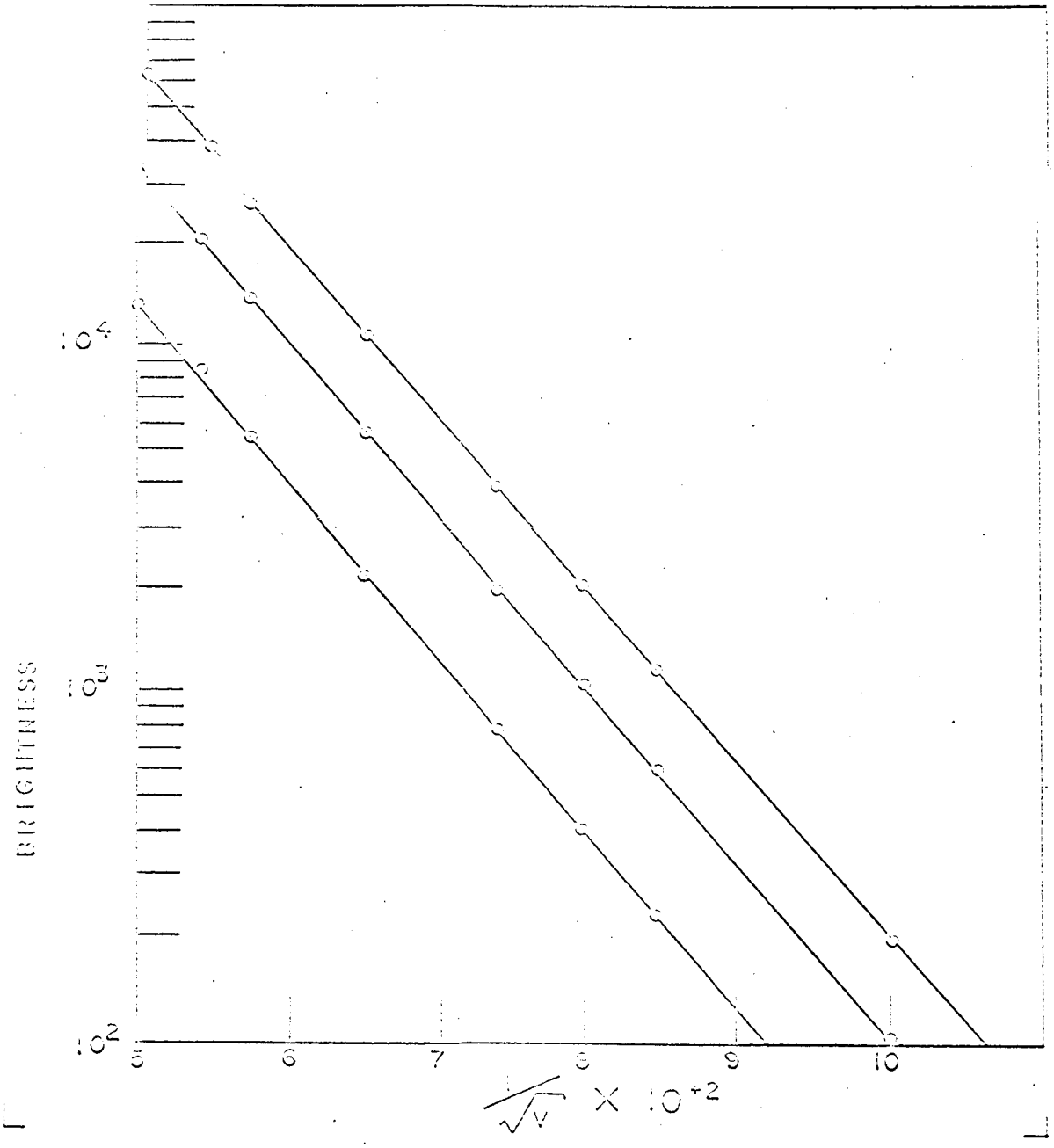

Figure 8

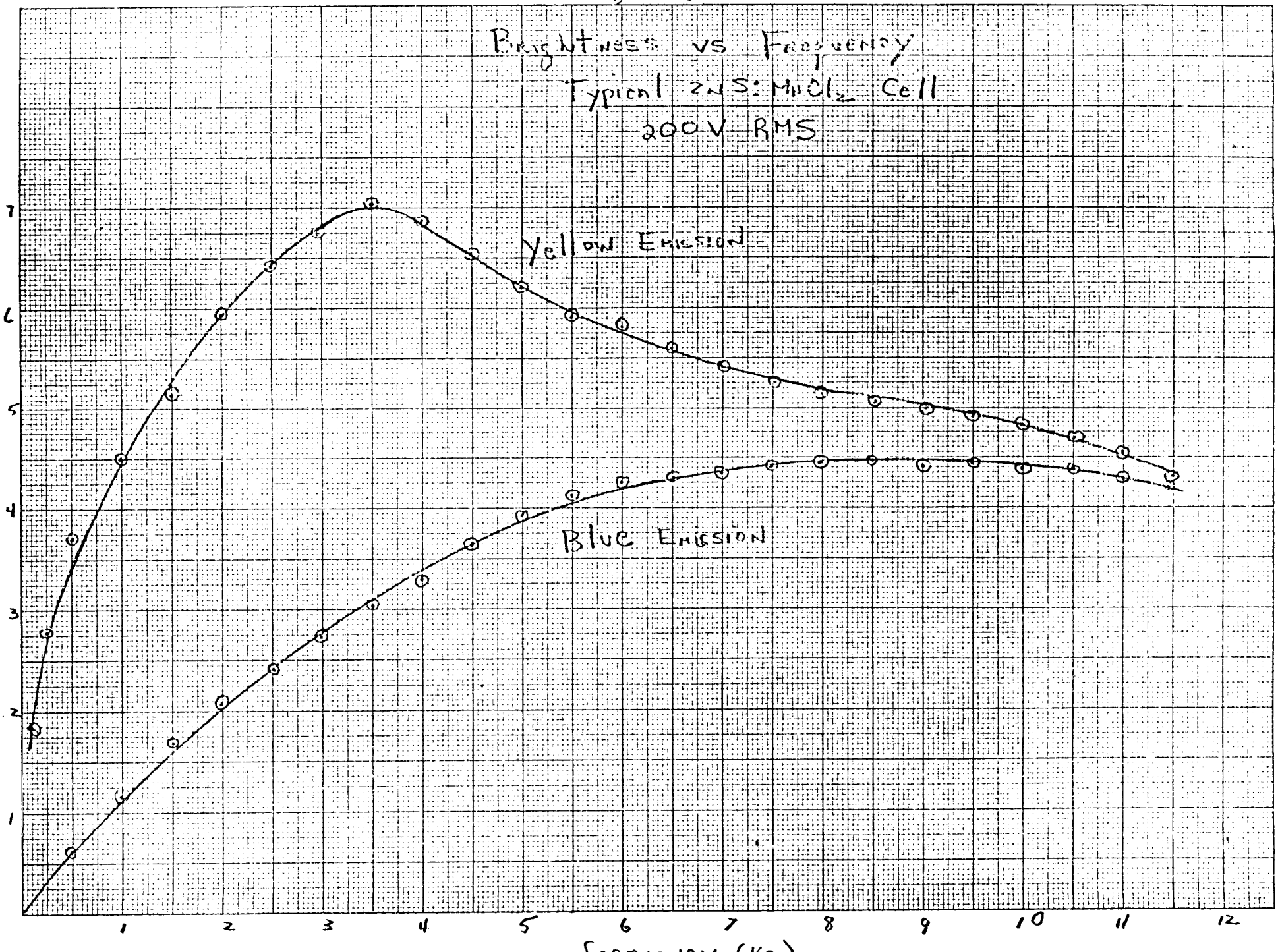

Figure 9

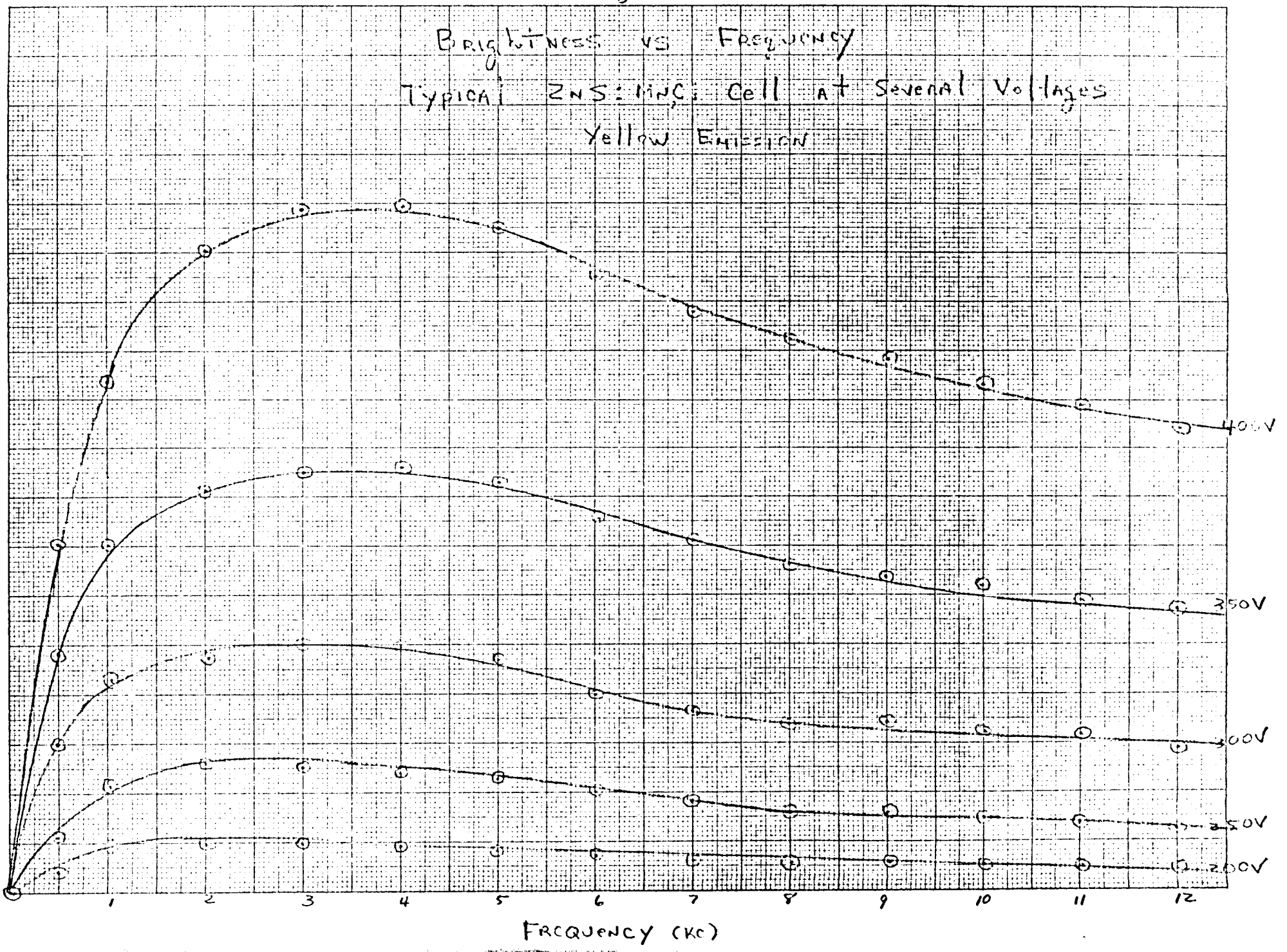

Figure 10

Block Diagram of Apparatus for Brightness Wave Measurements

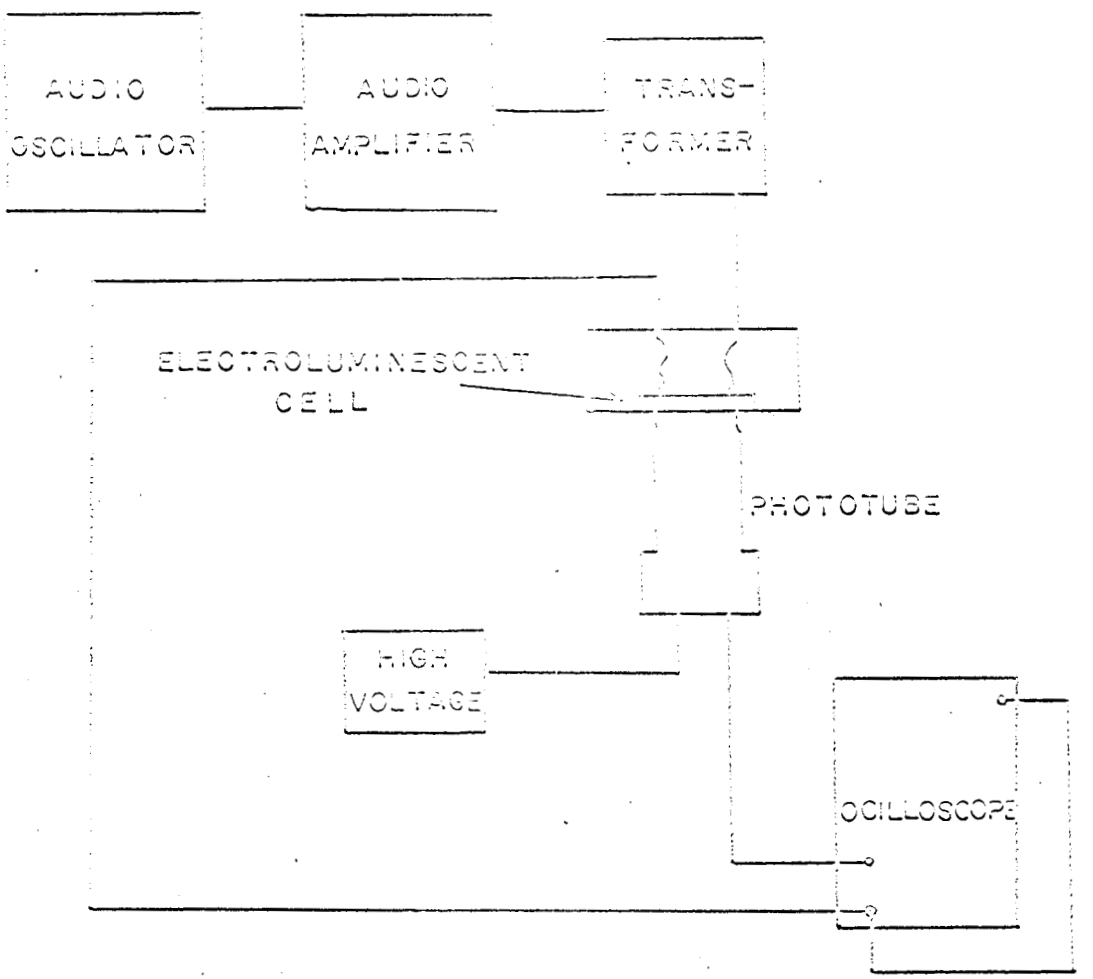

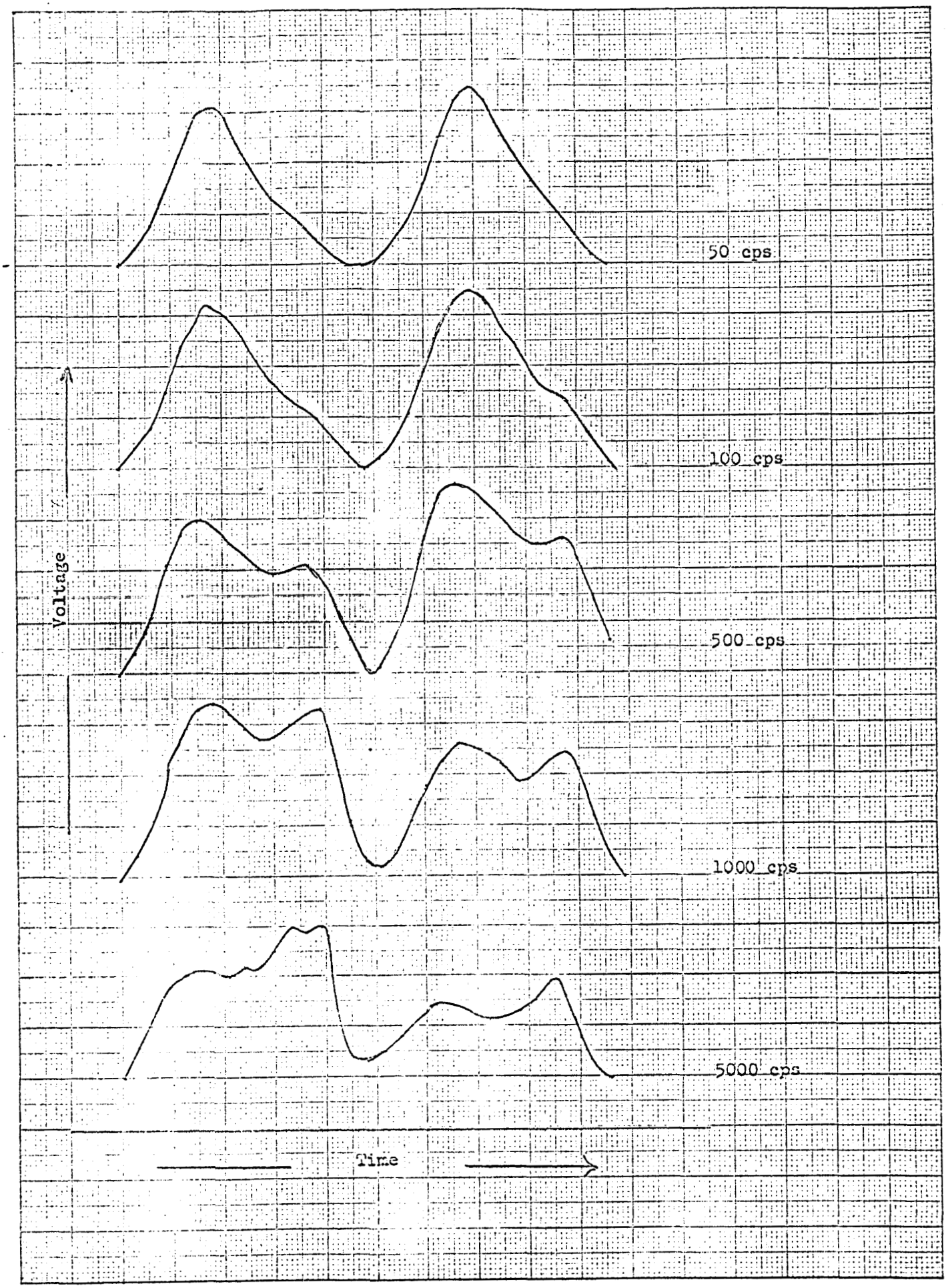

Figure 11
Brightness Waves as Functions of Frequency

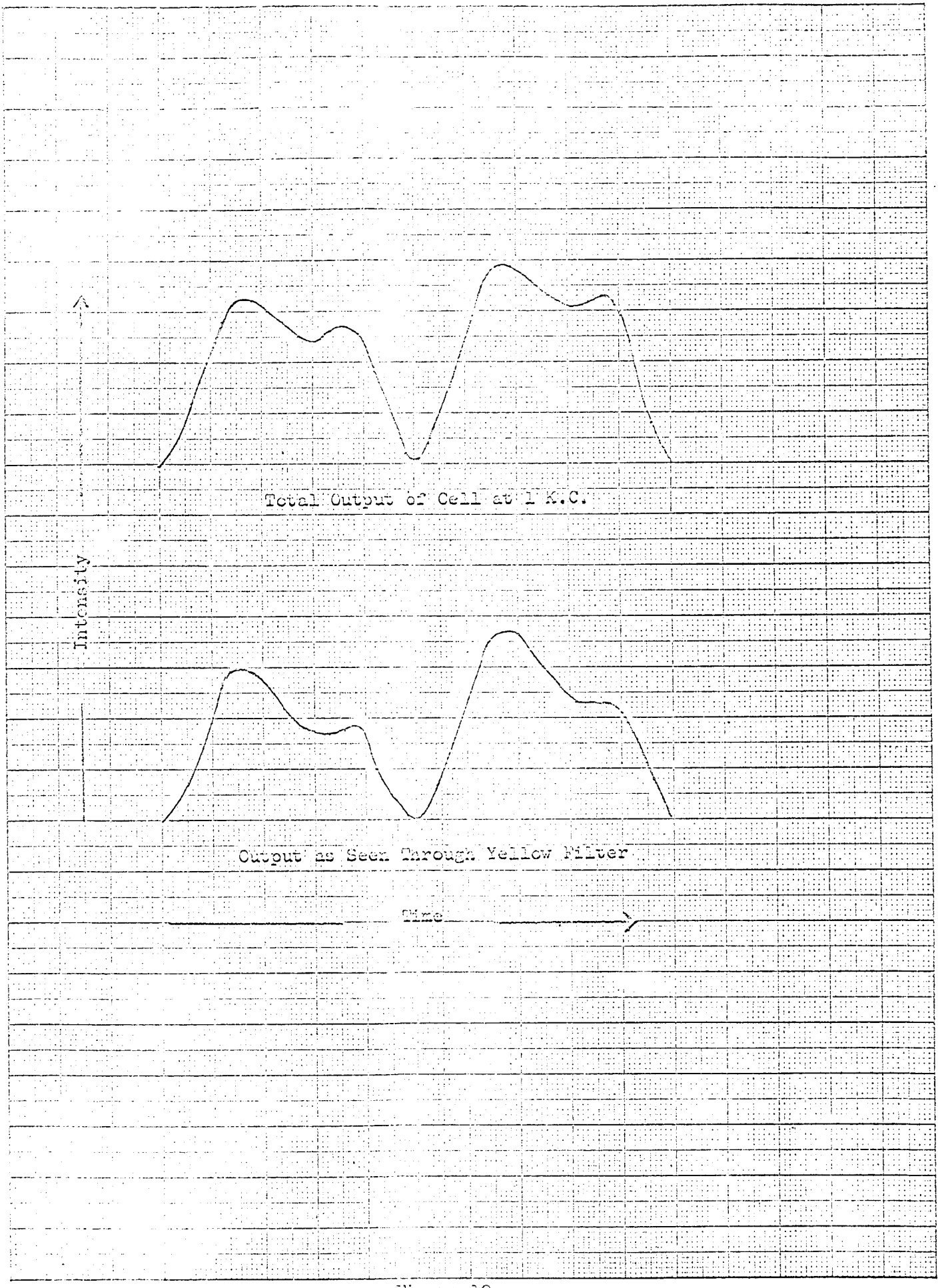

Figure 12
Brightness Waves Showing Predominance of Blue Emission in Secondary Peak

Figure 13

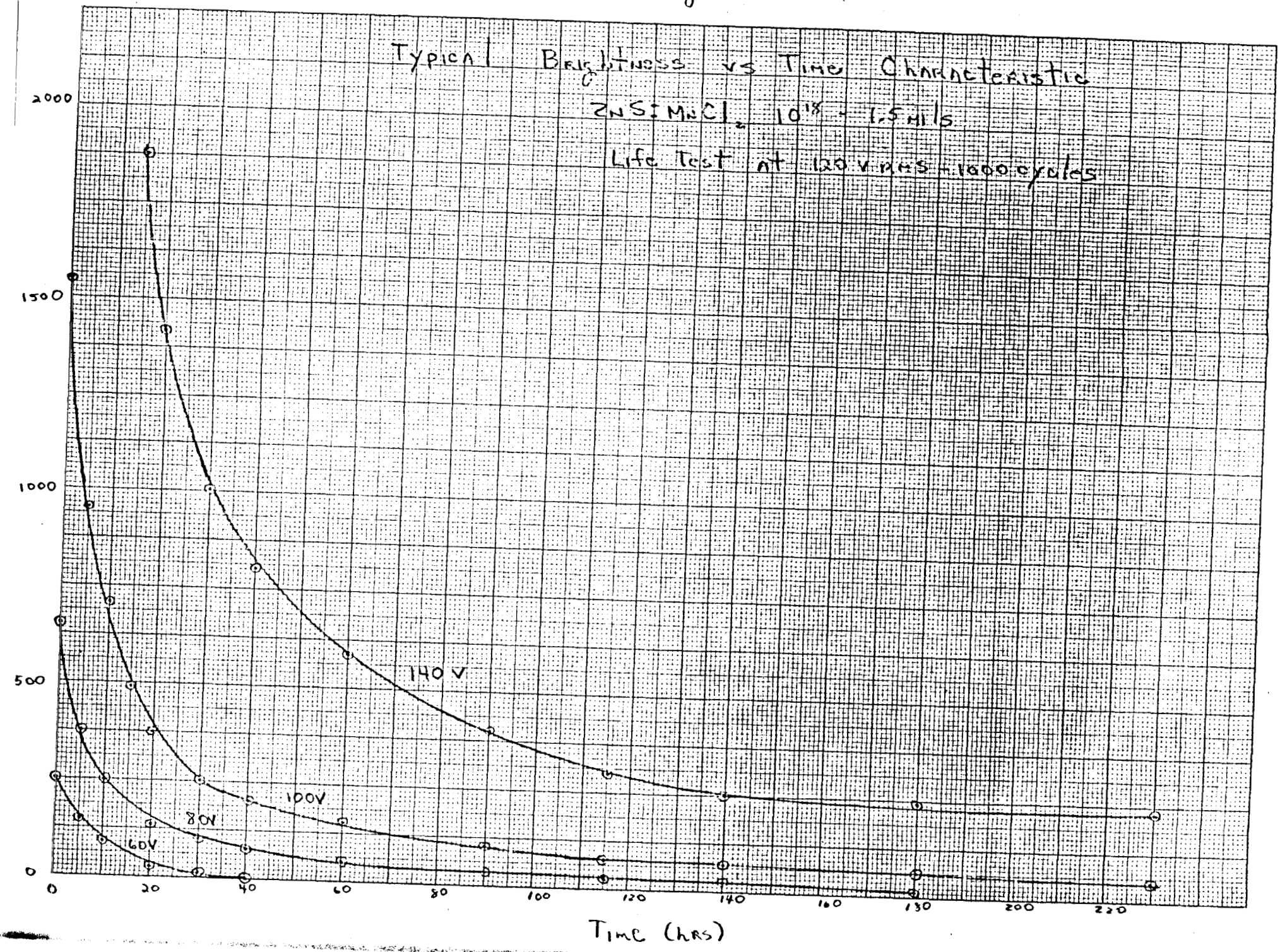

Figure 14

Brightness vs. Time for Cells
of Varying Thickness

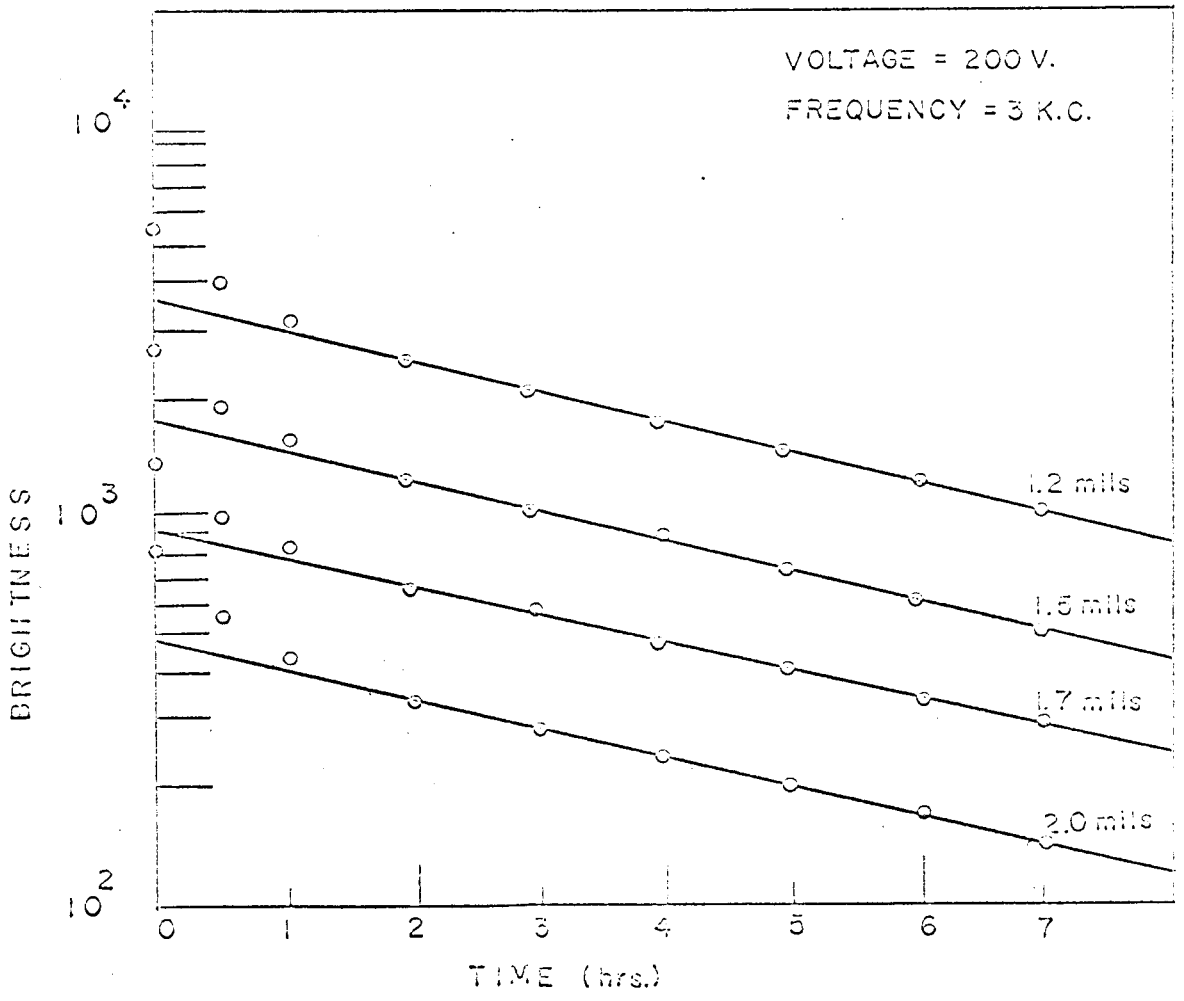

Figure 15

Brightness vs. Time as a
Function of Frequency

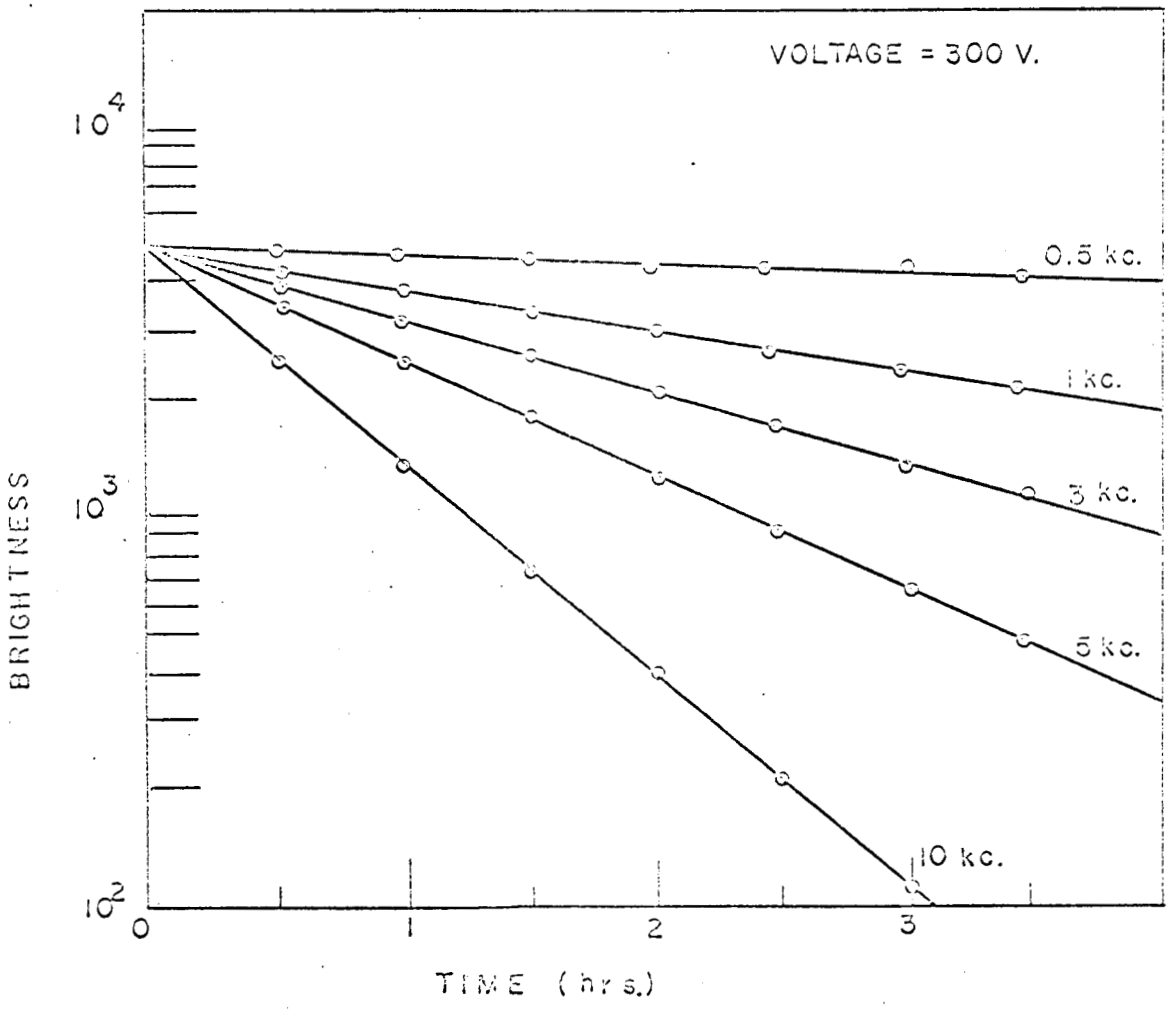

Figure 16

Half-life of Brightness vs. Frequency
as a Function of Impurity
Concentration

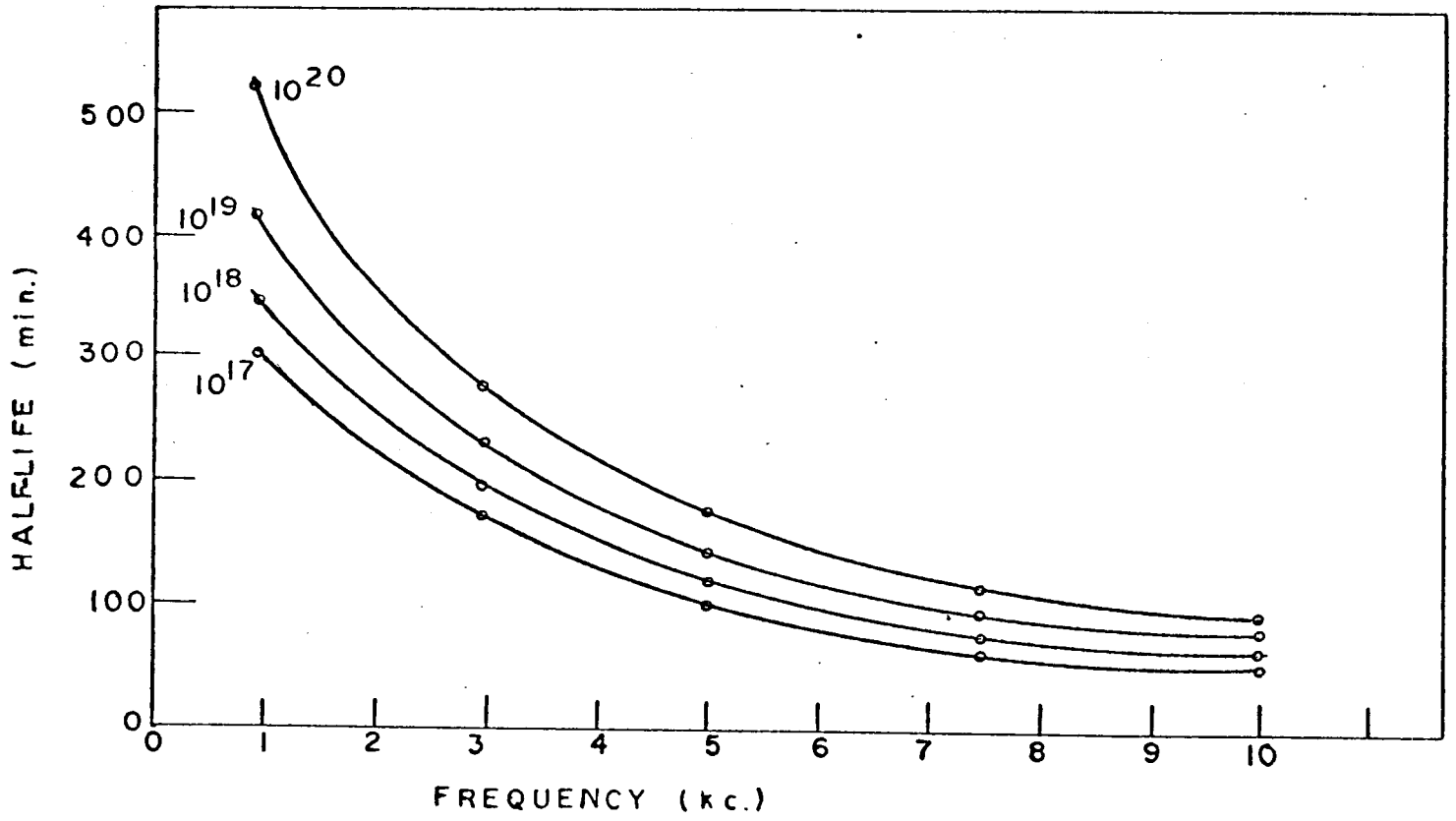

Figure 17

Block Diagram of Apparatus
for Relaxation Time
Measurements

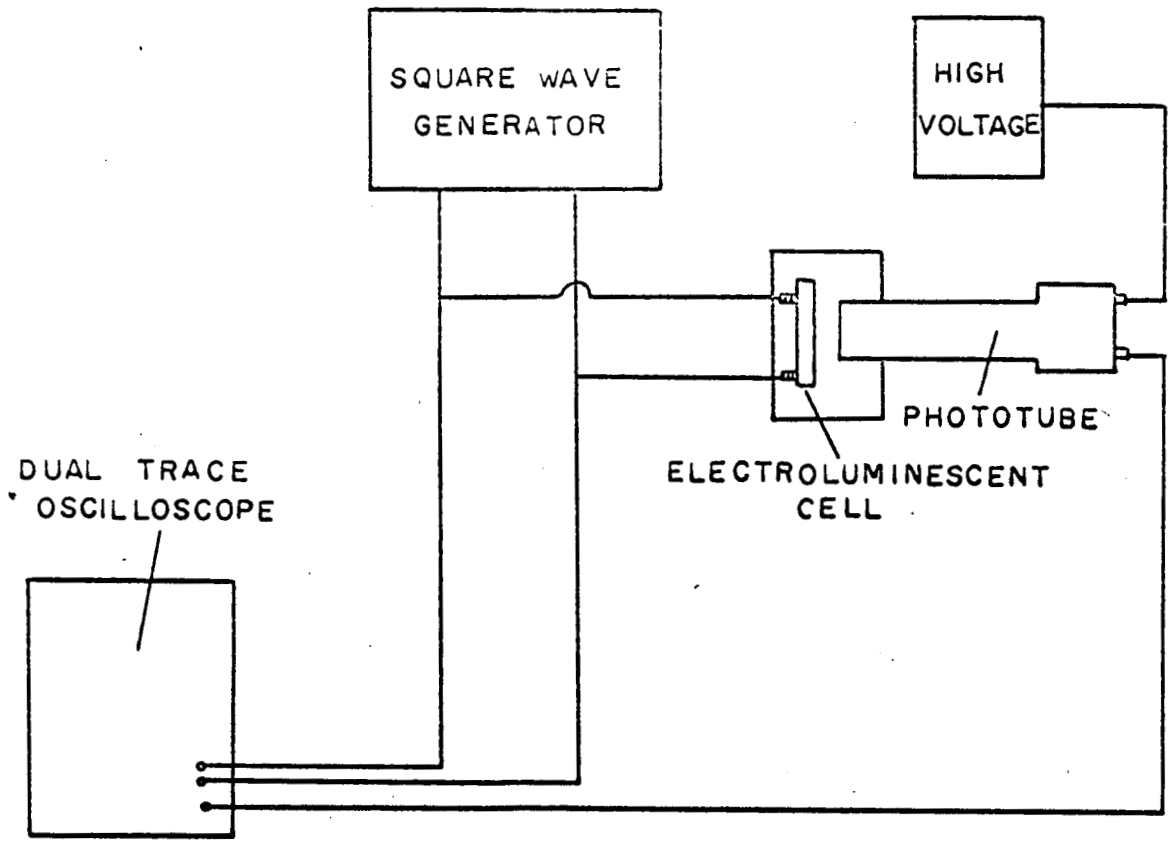

Figure 18

Decay of Brightness upon Removal
of Square Wave Voltage

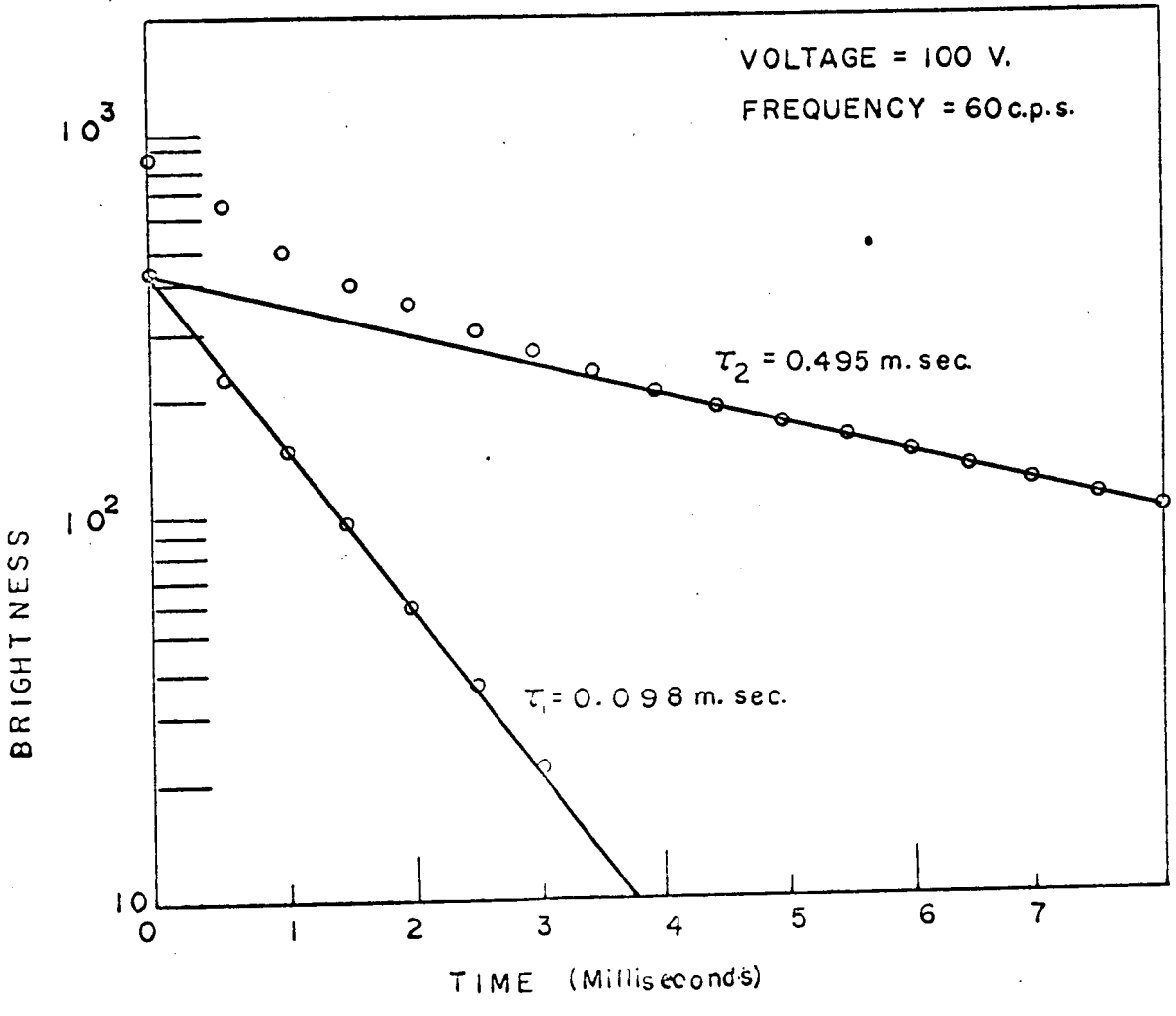

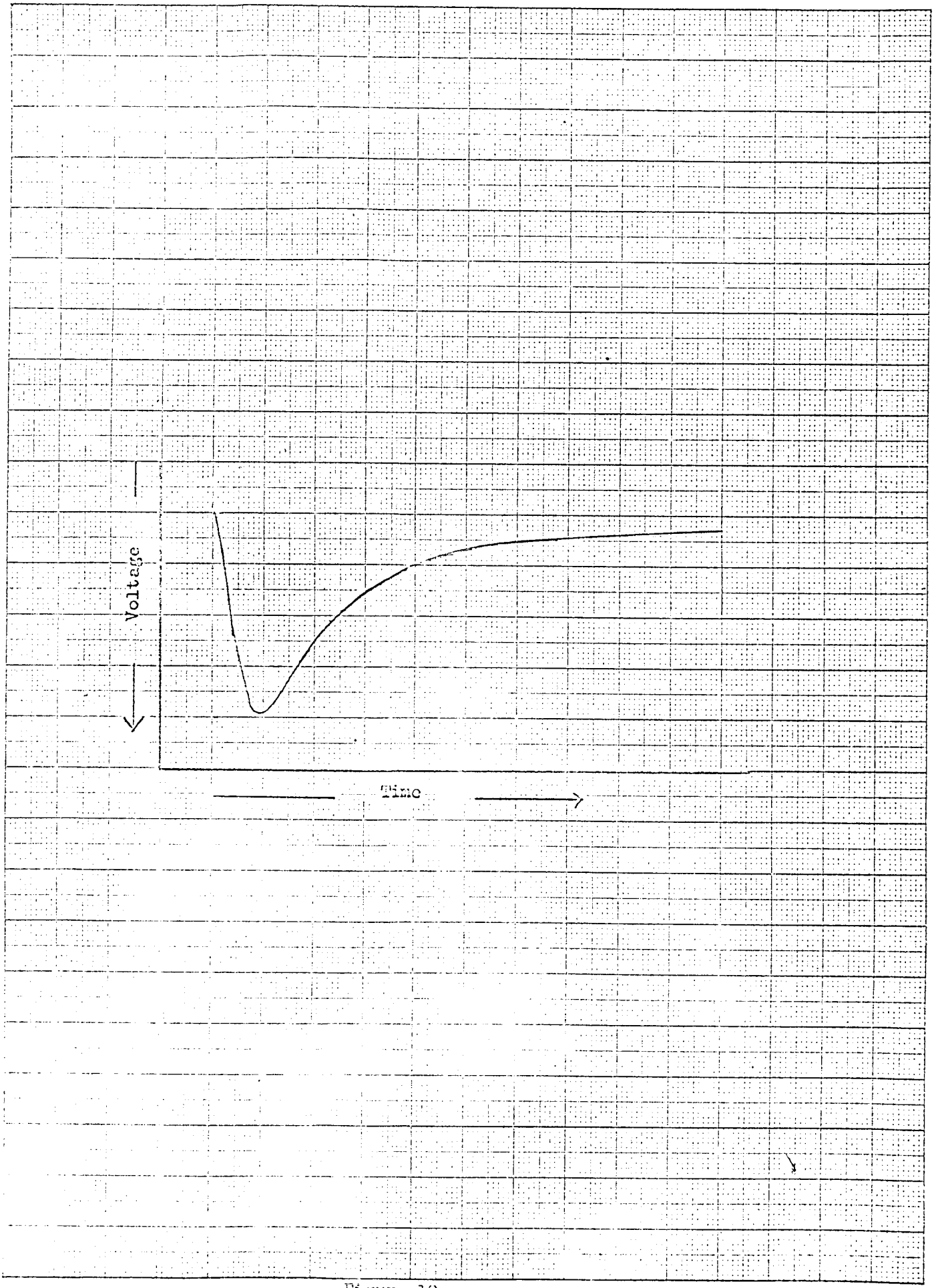

Figure 19

Typical Buildup and Decay of Light Output After Removal of Square Wave Voltage

Figure 20

Relative Efficiency vs. Frequency
as a Function of Voltage

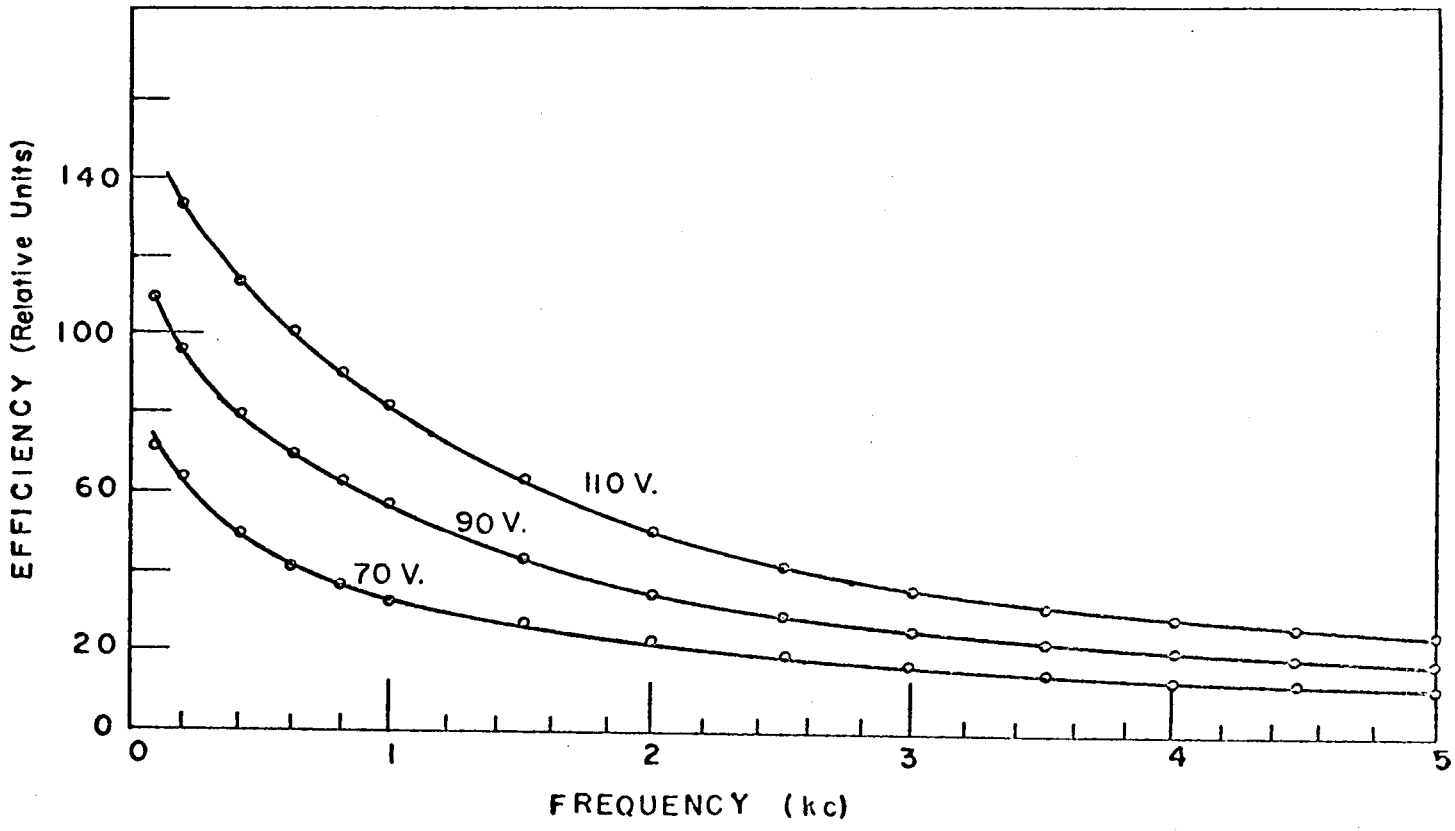

Figure 21

Block Diagram of Apparatus for
Absolute Efficiency Measurements

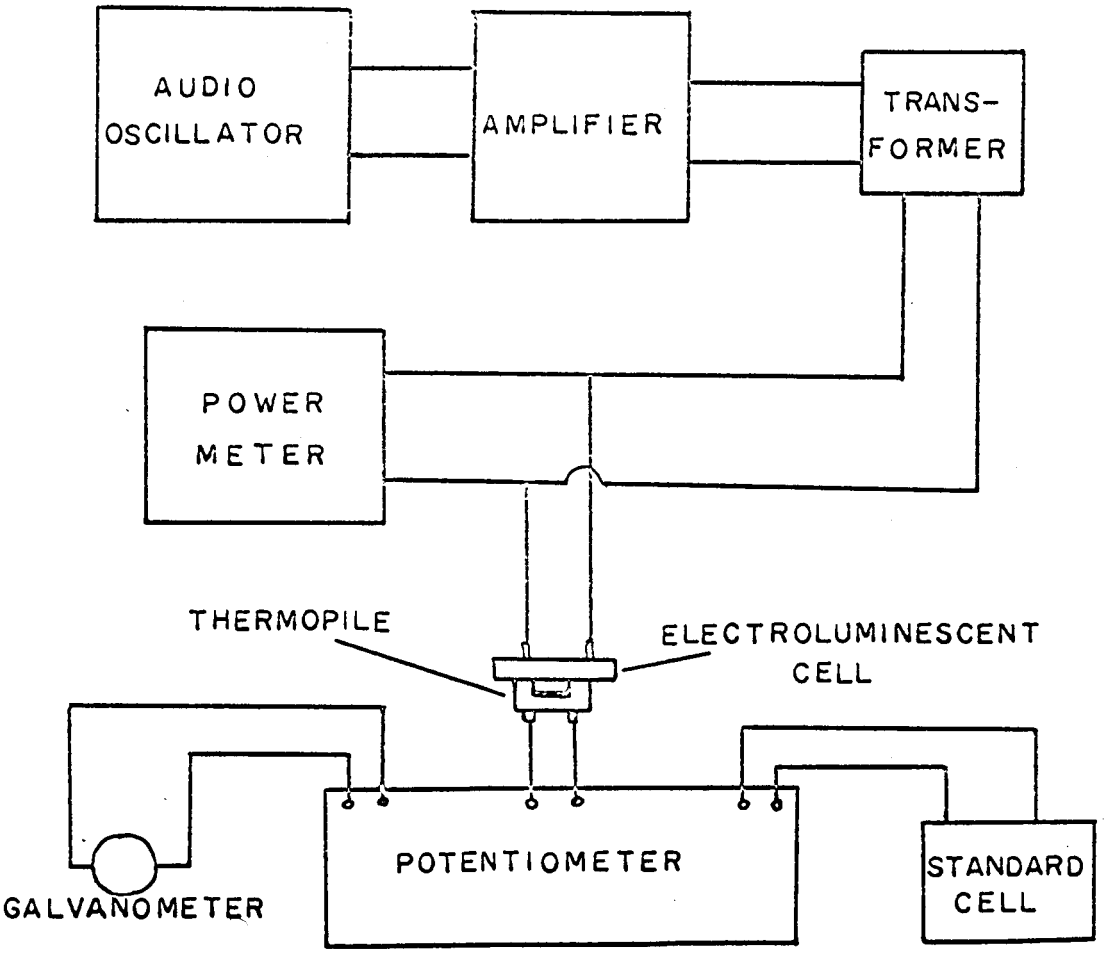

Figure 22

Cell Current vs. Frequency as a
Function of Applied Voltage

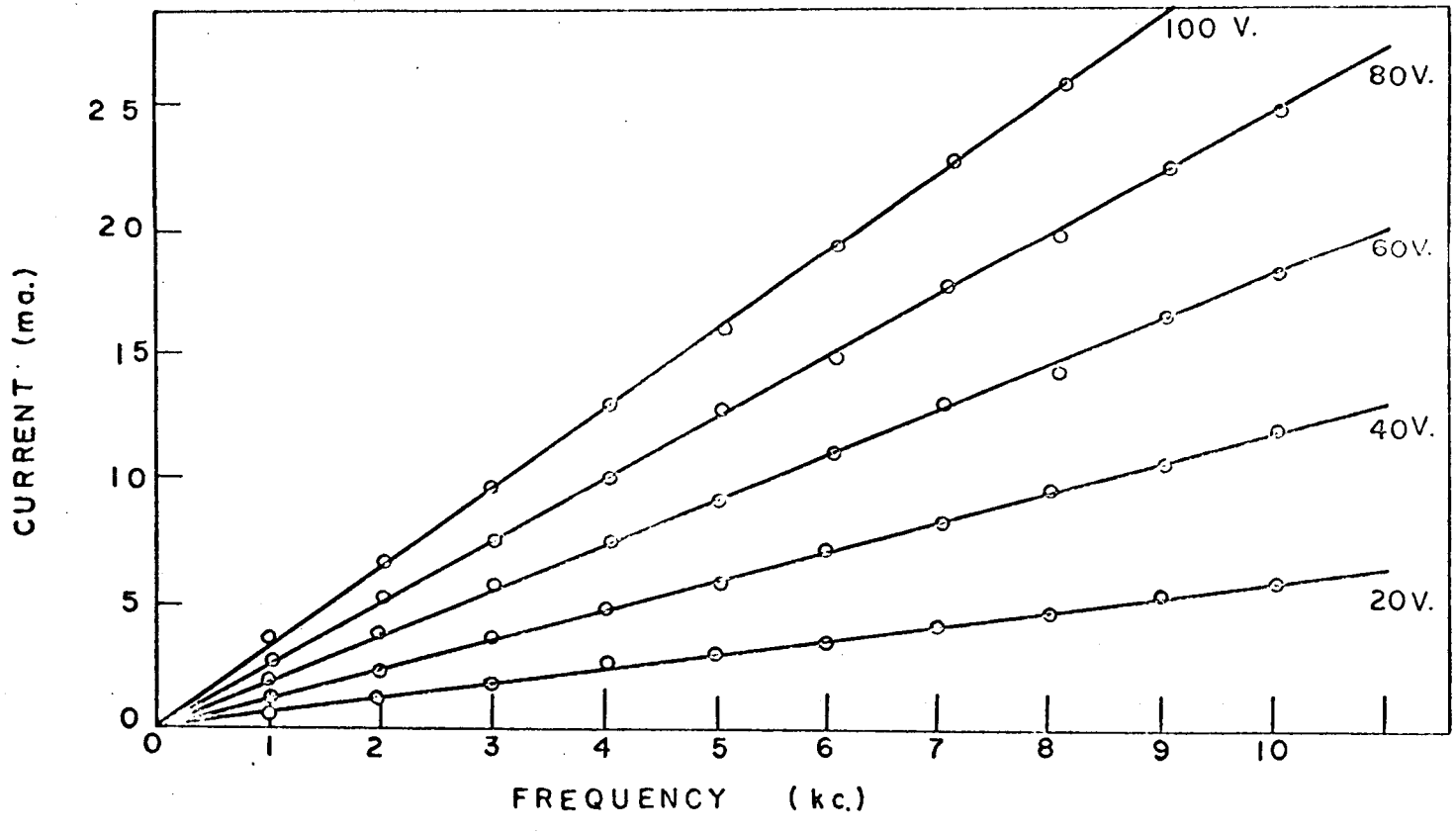

Figure 23

Cell Input Power vs. Voltage
for Various Frequencies

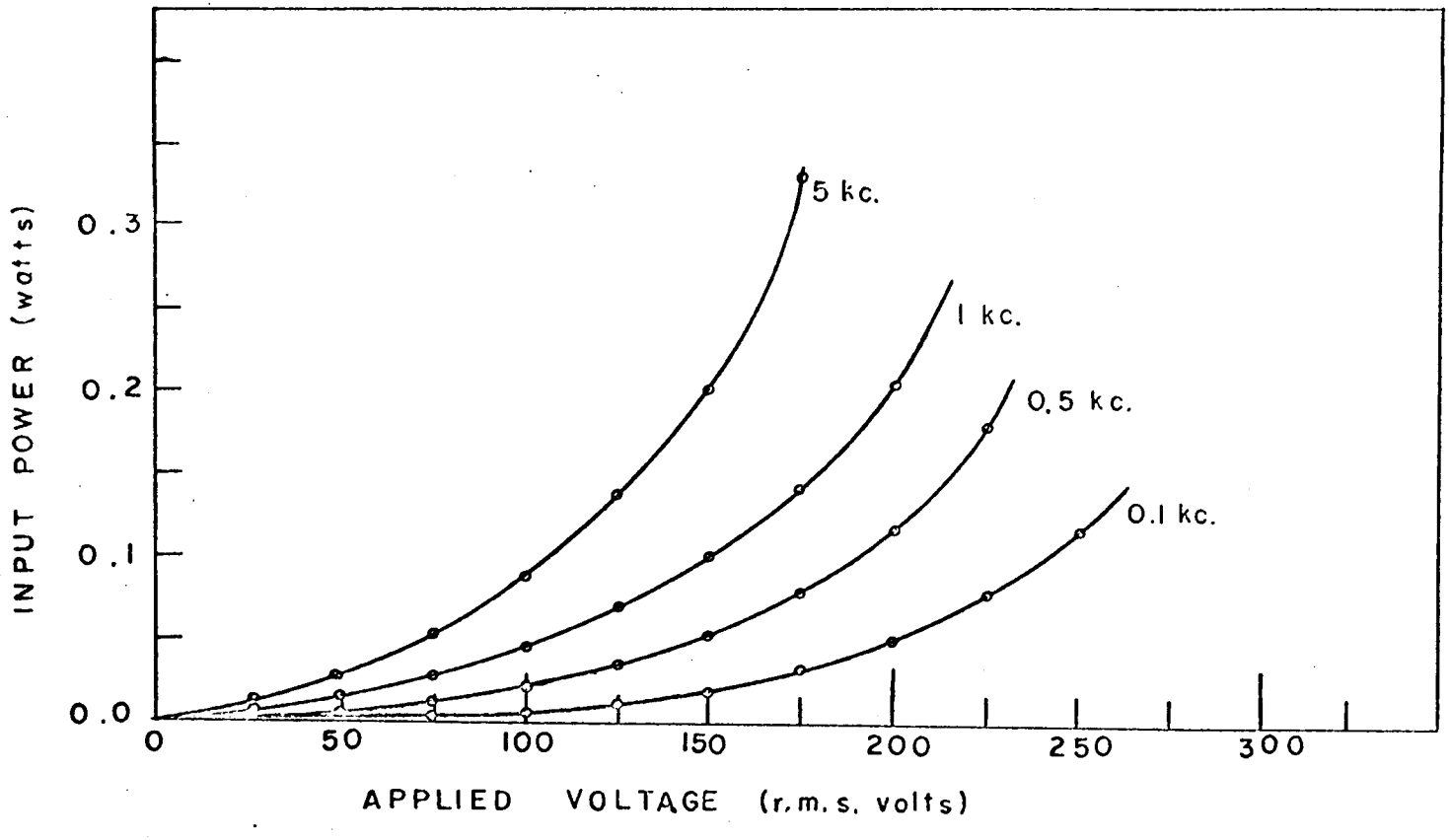

Figure 24

Composite Band Theory Picture
of Electroluminescence

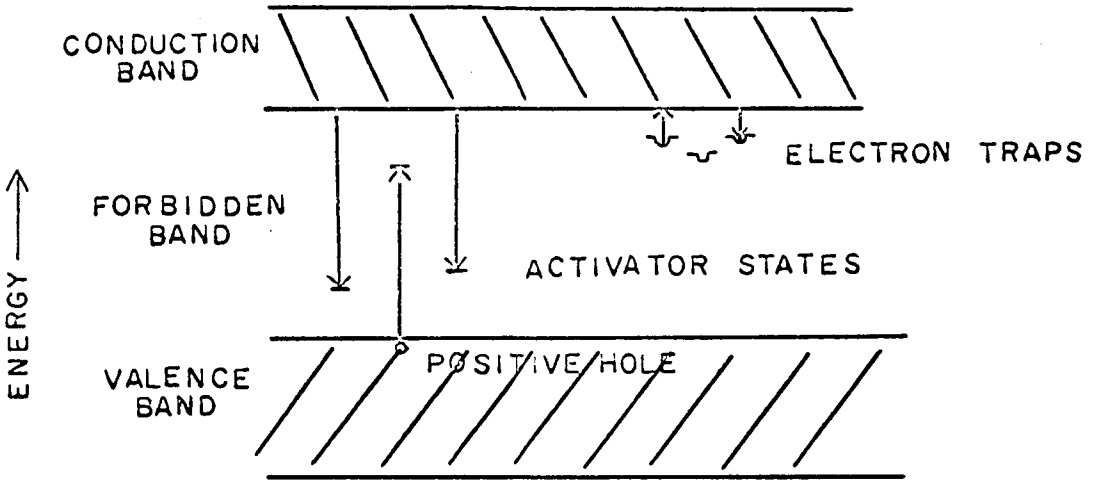

Figure 25

Configuration Coordinate Diagram
of Luminescence

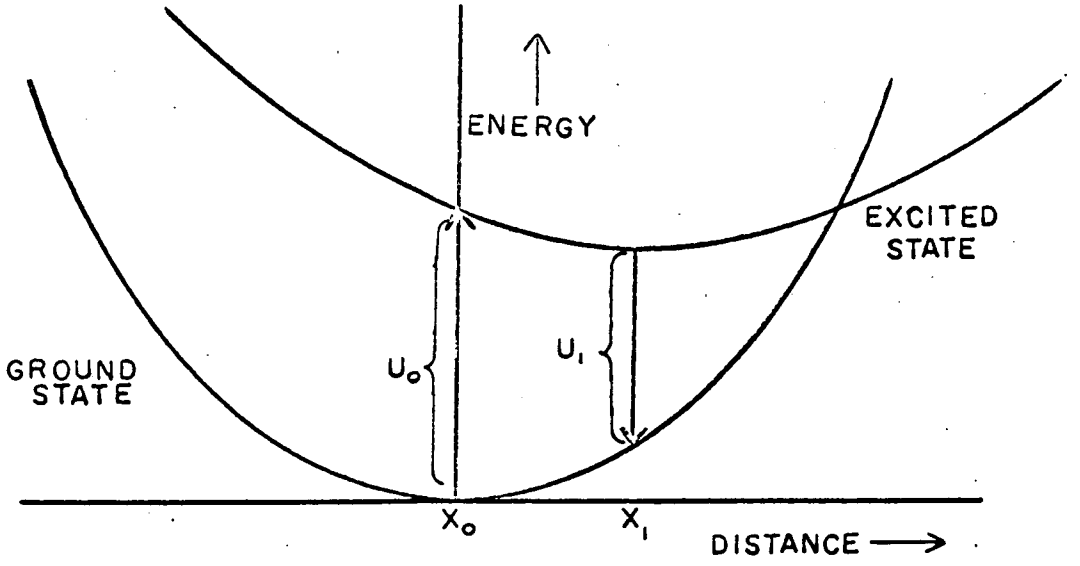

Figure 26

Energy Level Structure of ZnS:Mn
Assuming Perturbation of
$3d^5$ States by Crystalline
Field

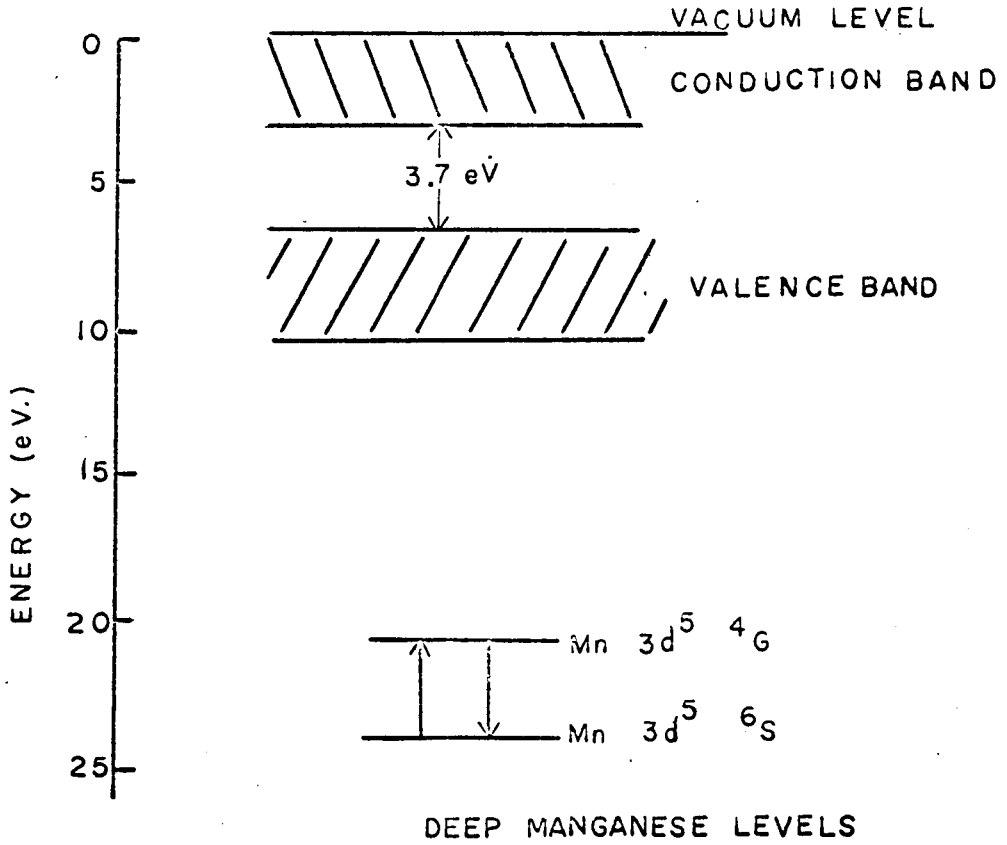

Figure 27

Configuration Coordinate Diagram of
Mn^{++} Luminescent Center

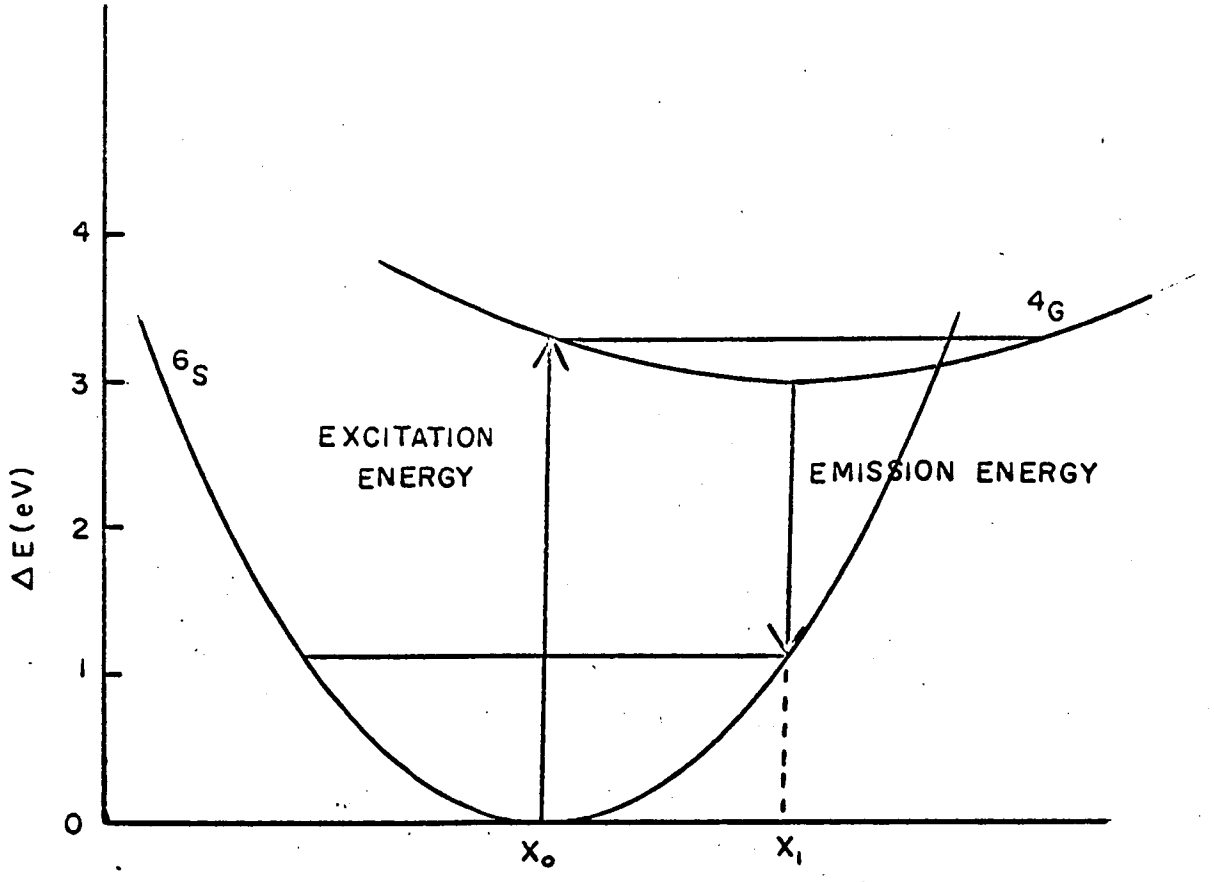

Figure 28

Curve Fit of Brightness vs. Time
Data for Blue Emission

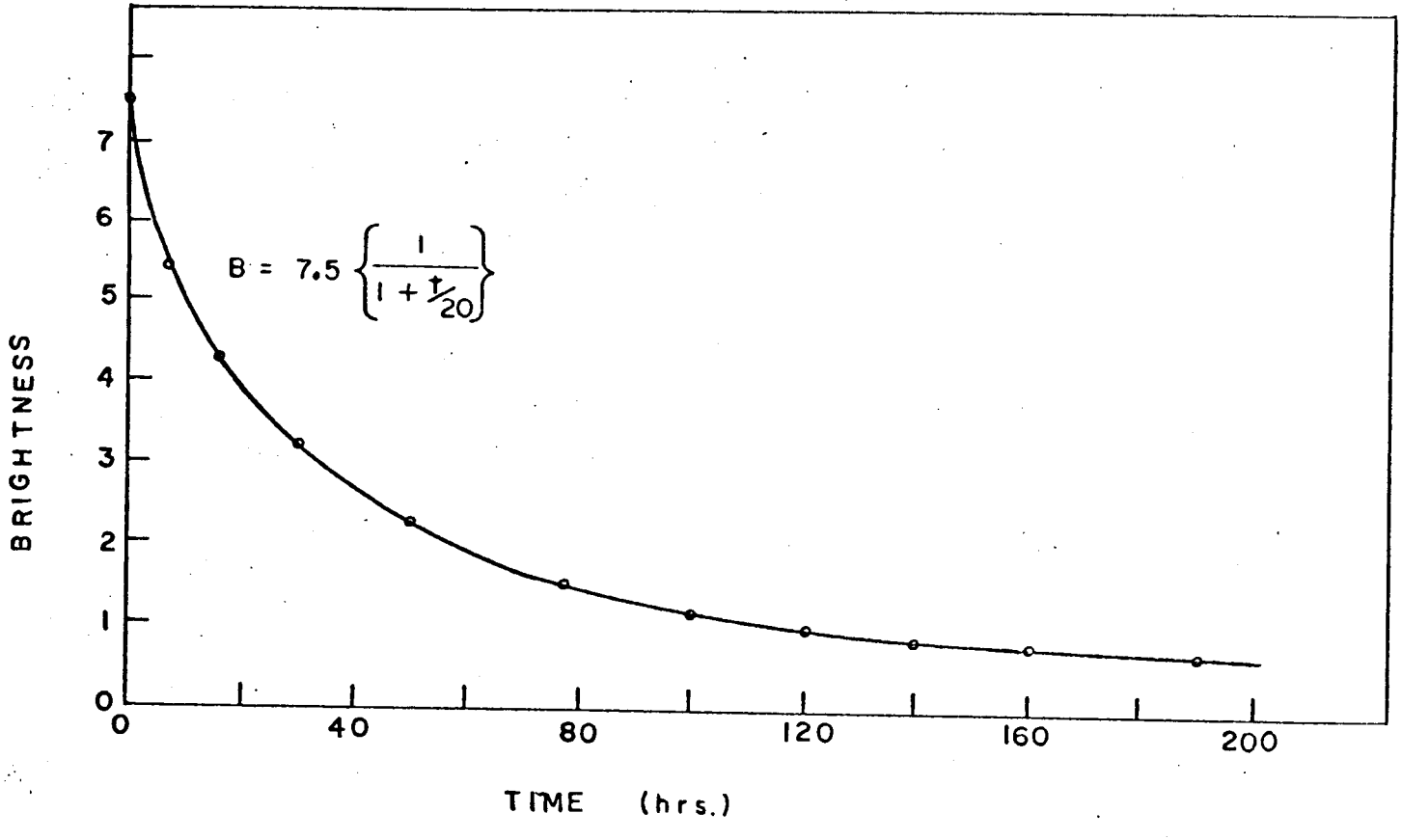

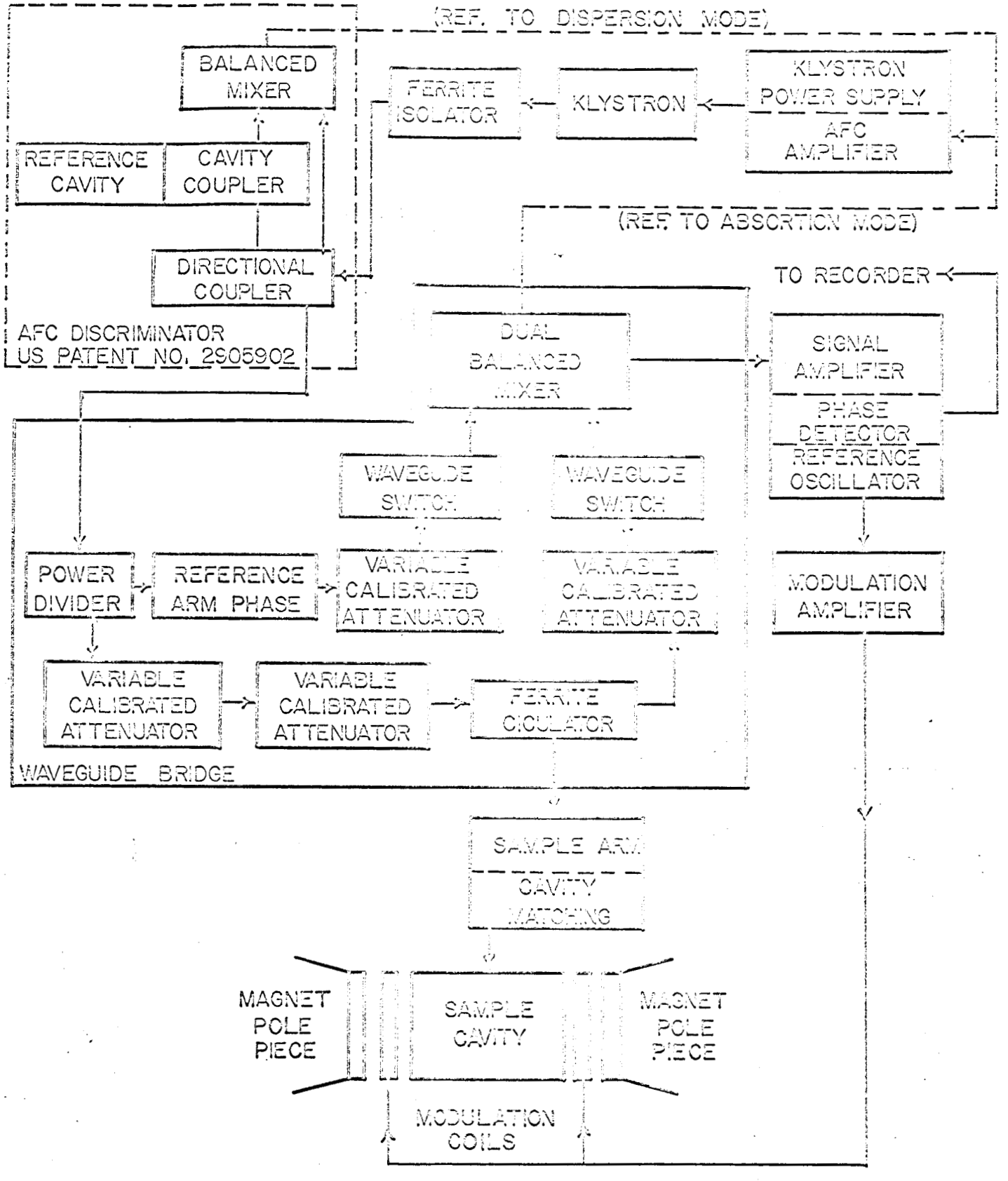

FIG. 29. BLOCK DIAGRAM OF THE STRAND L.A.B. MODEL 602 E.P.R. BRIDGE

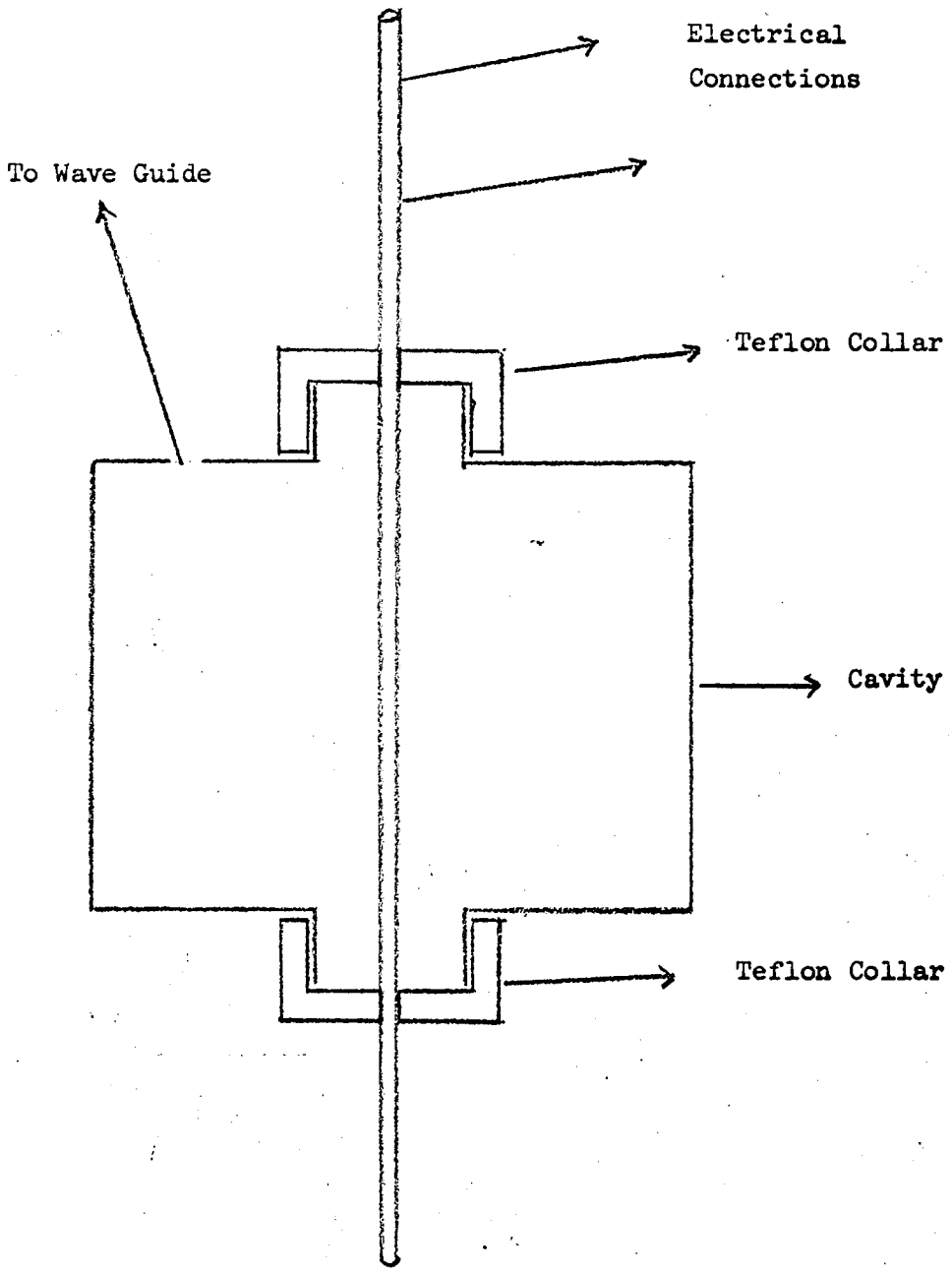

Cavity and Wire

Figure 29a

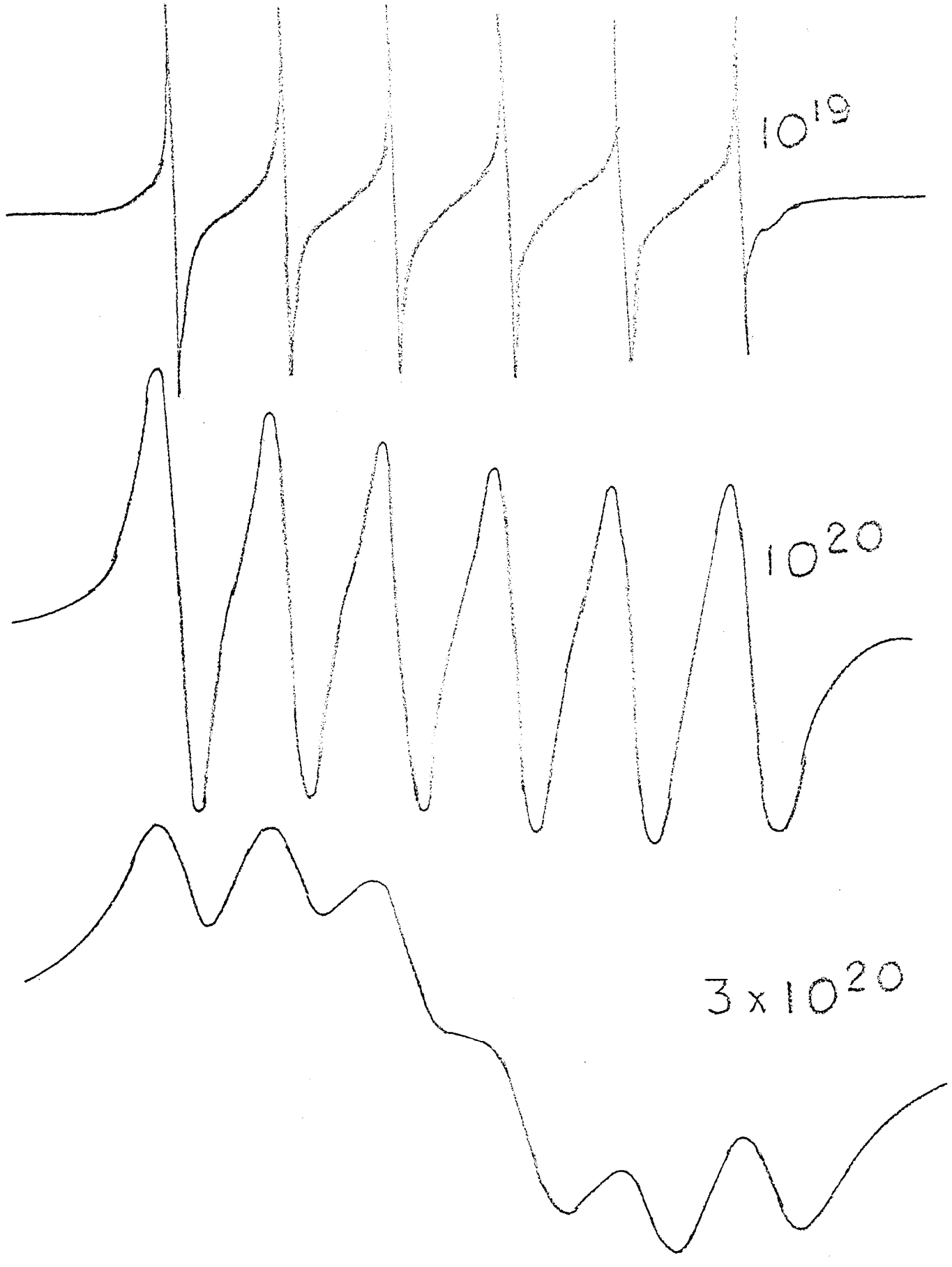

EPR Signal as Function of Concentration

Figure 30

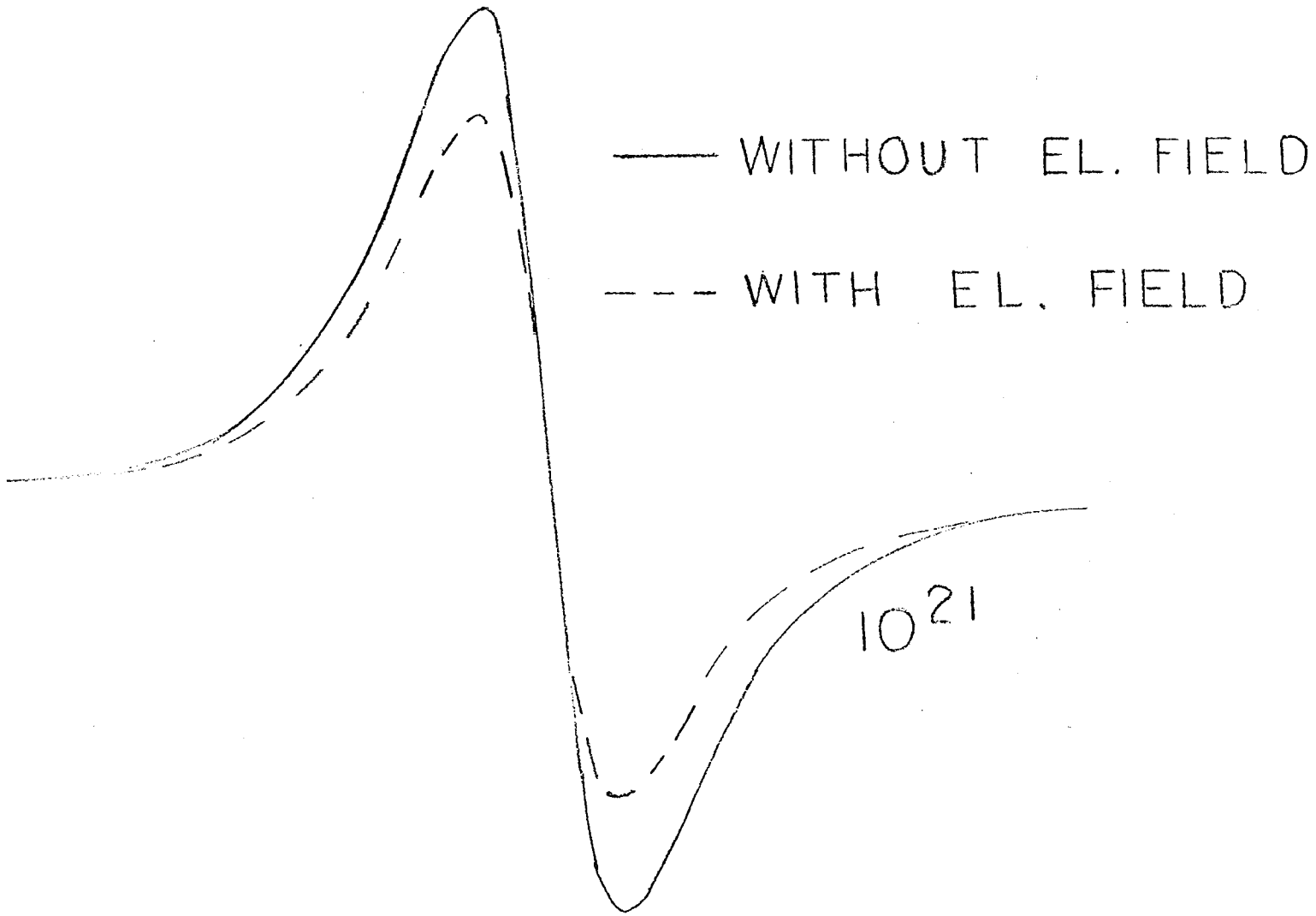

EPR Signal With and Without E.L. Field

Figure 31

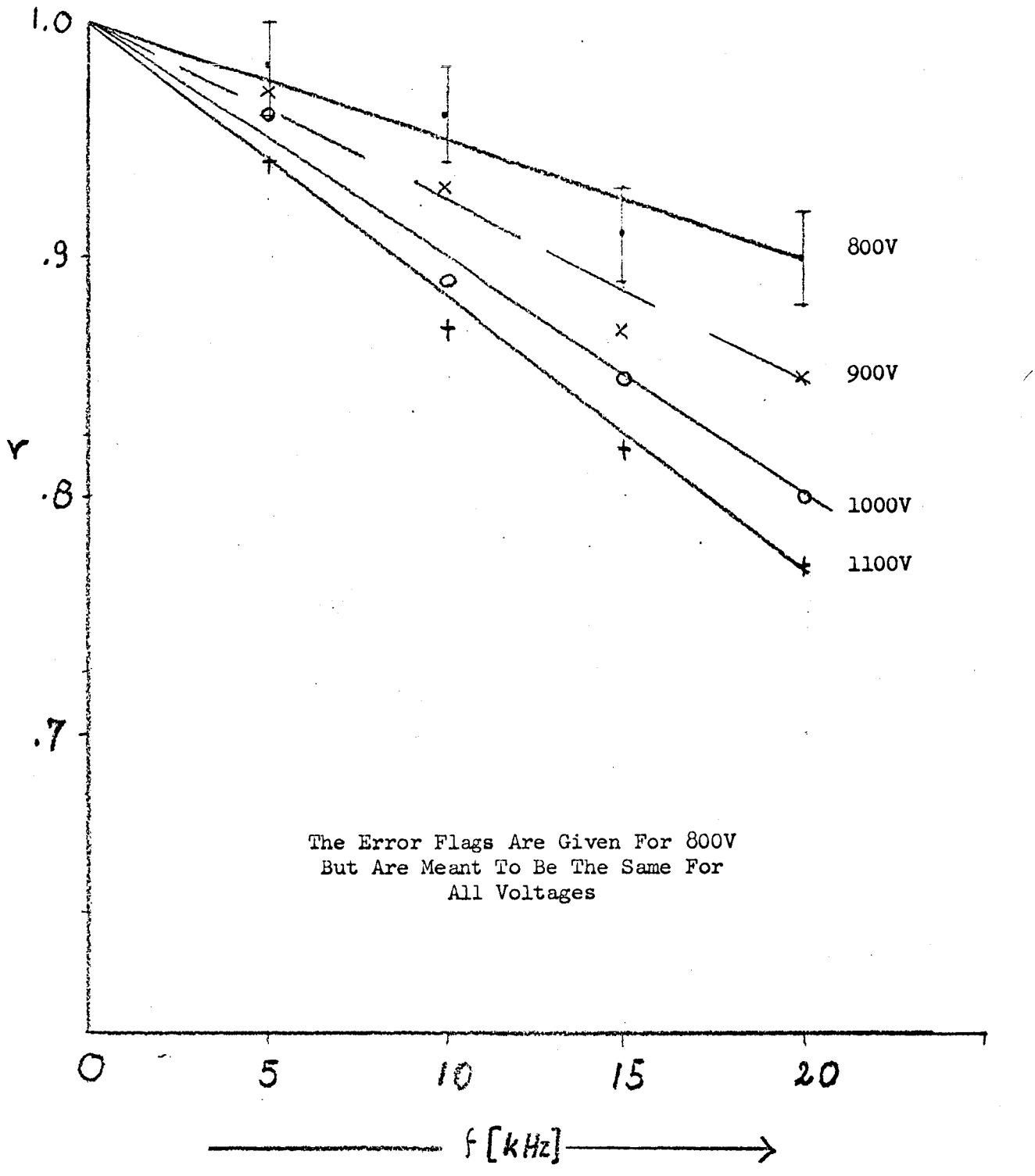

r As A Function Of Frequency

Figure 32